Harmful Algae 126 (2023) 102435

Contents lists available at ScienceDirect

Harmful Algae

journal homepage: www.elsevier.com/locate/hal

A cross-regional examination of patterns and environmental drivers of *Pseudo-nitzschia* harmful algal blooms along the California coast

Marco Sandoval-Belmar [a,*], Jayme Smith [b], Allison R. Moreno [a], Clarissa Anderson [c], Raphael M. Kudela [d], Martha Sutula [b], Fayçal Kessouri [a,b], David A. Caron [e], Francisco P. Chavez [f], Daniele Bianchi [a]

[a] Department of Atmospheric and Oceanic Sciences, University of California, Los Angeles, CA 90095-1565, United States of America
[b] Southern California Coastal Water Research Project, 3535 Harbor Blvd, Suite 110, Costa Mesa, CA 92626-1437, United States of America
[c] Southern California Coastal Ocean Observing System, Scripps Institution of Oceanography, La Jolla, CA, United States of America
[d] Ocean Sciences Department, University of California Santa Cruz, Santa Cruz, CA, United States of America
[e] Department of Biological Sciences, University of Southern California, 3616 Trousdale Parkway, Los Angeles, CA 90089-0371, United States of America
[f] Monterey Bay Aquarium Research Institute, Moss Landing, California, United States of America

ARTICLE INFO

Edited by Dr Holly Bowers

Keywords:
Domoic acid
Pseudo-nitzschia
Harmful algal blooms
California
Time series

ABSTRACT

Pseudo-nitzschia species with the ability to produce the neurotoxin domoic acid (DA) are the main cause of harmful algal blooms (HABs) along the U.S. West Coast, with major impacts on ecosystems, fisheries, and human health. While most *Pseudo-nitzschia* (PN) HAB studies to date have focused on their characteristics at specific sites, few cross-regional comparisons exist, and mechanistic understanding of large-scale HAB drivers remains incomplete. To close these gaps, we compiled a nearly 20-year time series of *in situ* particulate DA and environmental observations to characterize similarities and differences in PN HAB drivers along the California coast. We focus on three DA hotspots with the greatest data density: Monterey Bay, the Santa Barbara Channel, and the San Pedro Channel. Coastwise, DA outbreaks are strongly correlated with upwelling, chlorophyll-a, and silicic acid limitation relative to other nutrients. Clear differences also exist across the three regions, with contrasting responses to climate regimes across a north to south gradient. In Monterey Bay, PN HAB frequency and intensity increase under relatively nutrient-poor conditions during anomalously low upwelling intensities. In contrast, in the Santa Barbara and San Pedro Channels, PN HABs are favored under cold, nitrogen-rich conditions during more intense upwelling. These emerging patterns provide insights on ecological drivers of PN HABs that are consistent across regions and support the development of predictive capabilities for DA outbreaks along the California coast and beyond.

1. Introduction

Harmful algal blooms (HABs) are a significant threat to coastal ocean systems and are projected to worsen in a future climate (Howes et al., 2015; Trainer et al., 2012, 2020a; Wells et al., 2020). HABs are generated by multiple phytoplankton species, with cascading effects on marine ecosystems, human health, aquaculture, and coastal tourism (Trainer et al., 2000; Anderson et al., 2021). One of the most common HABs along the U.S. West Coast is caused by *Pseudo-nitzschia* spp. (PN), a diatom genus that produces the neurotoxin domoic acid (DA) (Bates et al., 1989; Lewitus et al., 2012). DA bioaccumulates in filter- and benthic feeding organisms and is transferred through the food web (McCabe et al., 2016; Bernstein et al., 2021). Human consumption of contaminated organisms can result in amnesic shellfish poisoning (Bates et al., 1989). Major cases of intoxication in humans have been documented (Perl et al., 1990). However, due to vigilant monitoring efforts by public health agencies, outbreaks are rare (Lefebvre and Robertson, 2010; Schnetzer et al., 2013). Nevertheless, DA-producing blooms have resulted in significant negative impacts on marine mammal and bird populations (Bejarano et al., 2008; Gibble et al., 2021; Moriarty et al., 2021), and have damaged local economies following closures of commercial, recreational, and Tribal fisheries (McCabe et al., 2016; Moore et al., 2020), thus underscoring the need for continuous monitoring and improved capacity to predict these events (Wells et al., 2020; Moreno

* Corresponding author.
E-mail address: marcsandovalb@atmos.ucla.edu (M. Sandoval-Belmar).

https://doi.org/10.1016/j.hal.2023.102435
Received 6 January 2023; Received in revised form 5 April 2023; Accepted 16 April 2023
Available online 26 April 2023

et al., 2022).

Along the California coast, several subregions are characterized by intense and recurring DA events, and are thus considered "DA hotspots" (Fig. 1; Trainer et al., 2012; Bates et al., 2018; Wood et al., 2017). Among them, Monterey Bay (MB) has been the focus of several studies on the dynamics of DA events (Lane et al., 2009; Cochlan et al., 2008; Timmerman et al., 2014; McCabe et al., 2016; Ryan et al., 2014; 2017). Long residence times and enhanced stratification (Graham, 1993) have been suggested as factors supporting distinctive PN populations (Bowers et al., 2018) and promoting toxic blooms within the Bay (Ryan et al., 2014). Further south, in the Southern California Bight (herein Bight), two DA hotspots exist in Santa Barbara Channel (SBC) and San Pedro Channel (SPC) (Smith et al., 2018a). These two regions are somewhat protected from the main wind-driven upwelling that characterizes the central California coast. Periods of strong upwelling in SBC and SPC, on a relative basis, generally correspond to intermediate or weaker upwelling in central California (Anderson et al., 2006; Hickey *et al.* 1992; Smith et al., 2018a). The distinct physical dynamics of the Bight are influenced by the orientation of the coast (Anderson et al., 2006), and the presence of the Channel Islands and capes, which enhance small-scale circulation and nutrient supply (Kessouri et al., 2022). In SBC, upwelling and convergent cyclonic eddies favor accumulation and retention of phytoplankton and organic particles (Harms and Winant, 1998; Brzezinski and Washburn, 2011), while large-scale climatic shifts affect temperature and nutrient supply (Barron et al., 2013; Sekula-Wood et al., 2011). In SPC, which we define here as the Santa Monica and San Pedro Basins, upwelling and phytoplankton blooms are favored during periods of strong equatorward winds between February and May, and variable winds in the summer (Hickey *et al.* 1992; Smith et al., 2018a). In this region, nitrogen inputs from urban wastewater can rival oceanic nitrogen from upwelling (Howard et al., 2014), contributing to coastal eutrophication (Kessouri et al., 2021a) (see Supplementary Table S1 for a list of rivers and wastewater outfalls inputs in the study region). Detectable DA concentrations have been observed annually since the early 2000s (Schnetzer et al., 2007), with significant interannual variability (observed concentrations have spanned four orders of magnitude, Smith et al., 2018a).

High spatial and temporal variability make it challenging to accurately predict HAB events in these hotspots (Schnetzer et al., 2013; Smith et al., 2018b). Statistical models of toxigenic PN blooms identify upwelling (+), temperature (-), salinity (+), chlorophyll-a (Chl-a, +/-), silicic acid ($Si(OH)_4$, -), nitrate (NO_3^-, +), and river discharge (-) as significant predictors (Fig.2; Lane et al., 2009; Anderson et al., 2006, 2009, 2011; Schnetzer et al., 2007; 2013; Seubert et al., 2013; Smith et al., 2018a,b). However, *in situ* data have not always yielded strong correlations and consistent directional relationships in California. Cooler temperatures and higher salinity are direct consequences of upwelling, a primary driver of toxigenic PN blooms (Lelong et al., 2012; Trainer et al., 2010; 2012; Smith et al., 2018b; Bates et al., 2018). Nevertheless, negative correlations between silicic acid concentrations and DA (Fig.2) are consistent with a post-upwelling nutrient regime where dissolved silicic acid has been drawn down by a diatom-dominated assemblage (Anderson et al., 2008) and acts as a regulating but not limiting nutrient (Kudela and Dugdale, 2000).

Laboratory experiments have shown that PN can take up both inorganic and organic nitrogen (Cochlan et al., 2008; Howard et al., 2007), suggesting that coastal nitrogen inputs could sustain PN communities during periods of weak upwelling and heavy runoff (Kudela et al., 2008). However, Smith et al. (2018b) found negative correlations between DA events and ammonium and urea for specific years (2013 and 2014). Other experiments with PN strains from California have pointed to iron deficiency (Maldonado et al., 2002; Wells et al., 2005; Ryan et al., 2014) and high pCO_2 as factors that could promote DA production (Tatters et al., 2012; Wingert and Cochlan, 2021).

Large-scale climatic patterns can also affect PN HABs. The most influential climate modes in the California Current are the Pacific Decadal Oscillation (PDO), North Pacific Gyre Oscillation (NPGO) and El Niño-Southern Oscillation (ENSO) (McCabe et al., 2016; McKibben et al., 2017; Sekula-Wood et al., 2011; Smith et al., 2018a). A positive PDO phase is related to warmer waters, suppresses upwelling, and reduces productivity (Mantua and Hare, 2002; Mantua et al., 1997; Henson and Thomas, 2007; Catlett et al., 2021), with opposite patterns during a negative phase. Positive phases of NPGO are related to an increase in the southward transport of the California Current, and more intense upwelling (Di Lorenzo *et al.*, 2008). During El Niño, conditions shift to weaker upwelling, warmer temperatures, and reduced nutrient supply and productivity, while opposite conditions usually characterize La Niña (Chavez et al., 2002; Jacox et al., 2015).

Comparative studies from DA-prone regions are essential to document the biogeography of events, and to establish robust indicators of HABs beyond local complexities (Wells et al., 2020) – a necessary foundation for models of PN HABs (Anderson et al., 2011, 2016; Moreno et al., 2022). However, comparative long-term analyses across DA regional hotspots remain rare. The goal of this study is to identify coastwide patterns and drivers of DA-producing HABs and their subregional variability. To address this goal, we conducted a comparative analysis between the three data-rich DA hotspots, using a >18-years observational record to shed light on: (1) The magnitude and typical seasonal cycle of DA events across the three regions; (2) The environmental conditions that enhance the probability of DA events and their strength, and the temporal lags that maximize the association between those variables; (3) The environmental thresholds associated with increased probability of DA detection; (4) The influence of low-frequency natural variability in promoting and sustaining DA events. With a remarkable wealth of observations, California is an ideal test bed for a comparative analysis of the drivers of PN HABs, guiding futures efforts for other regions. Based on the results, we highlight general patterns in PN HAB dynamics and propose a revised framework for the factors that favor the occurrence of DA event along the California coast and beyond.

2. Methods

This study is based on analysis of a large new compilation of particulate DA (pDA) measurements and co-located environmental variables along the California Coast. In the following sections, we detail the compilation, processing and quality control of the observational data, the generation of time series for each region, and the statistical approaches used for the analysis.

2.1. Dataset compilation

We compiled 14,451 *in situ* measurements of pDA from monitoring programs and independent research studies, including the California Harmful Algae Risk Mapping (C—HARM) model validation dataset (Anderson et al., 2016), consisting of 2329 coastwide stations sampled between 2000 and 2018, and an updated Southern California Bight dataset, covering the 2003–2020 period (Smith et al., 2018a). Although these datasets are rich in DA observations and generally include co-located hydrographic measurements, they both have gaps in ancillary information (*e.g.*, nutrients, Chl-a), especially in the early to mid-2000s. To fill these gaps, we compiled environmental data from several monitoring programs along the U.S. West Coast, including California Cooperative Oceanic Fisheries Investigations (CalCOFI), Monterey Bay Aquarium Research Institute (MBARI), Santa Monica Bay Observatory (SMBO), Plumes and Blooms (P&B) in SBC, The San Pedro Ocean Time series (SPOT), and other programs (see Supplementary Table S2). We also compiled daily river flows and monthly discharge flows from Publicly Owned Treatment Works (POTW) via ocean outfalls in the Southern California Bight (Supplementary Table S1), daily wind data from ERA5 Reanalysis, and key climatic indices including the PDO index, the Multivariate El Niño-Southern Oscillation index (MEI) and the

NPGO index. From the data, we derived several variables of interest, including proxies for nutrient ratios, such as Si* ($Si^* = Si(OH)_4 - NO_3^-$) and P* ($P^* = PO_4^{3-} - NO_3^- / 16$), which quantify the deficit of nitrate relative to silicic acid and phosphate (PO_4^{3-}), respectively, and a local Upwelling Index (UI) calculated as the wind speed component parallel to the coast (Supplementary Information).

2.2. Data processing and quality control

We consider observations from the upper 35 m as representative of the surface mixed layer depth for California during spring and summer (Renault et al., 2021; Kessouri et al., 2021b). Observations were gridded to an equally spaced horizontal grid and averaged as daily, weekly, and monthly time series starting in 2000 and ending in 2020 (Fig. 1 and Table 1). We removed outliers defined as values greater than three standard deviations above the mean for each variable, except for pDA. We generated weekly time series based on seven-day averages, using a geometric mean, plus one, for pDA to manage the zero-inflated skewed distribution (Eq. (1)), and a geometric mean to calculate Chl-a averages (Eq. (2)):

$$\overline{pDA} = \left[\sqrt[n]{(pDA_1 + 1) \cdot (pDA_2 + 1) \cdot (pDA_3 + 1) \ldots (pDA_n + 1)} \right] - 1 \quad (1)$$

$$\overline{Chl - a} = \sqrt[n]{(Chl_1) \cdot (Chl_2) \cdot (Chl_3) \ldots (Chl_n)} \quad (2)$$

One critical feature in our analysis was the definition of a "DA event" – *i.e.*, a measurement that detects significant pDA in the environment. Currently, there is no specific pDA concentration that defines an event, and DA quantification approaches used by monitoring programs and research studies typically have variable detection limits. Because we merged pDA observations from different studies, we set a common threshold of 0.05 $\mu g/l$ above which we consider the measurement reflective of a DA event. This value encompasses the lowest (0.01 $\mu g/l$) and highest (0.06 $\mu g/l$) detection limits reported in the literature (Schnetzer et al., 2007; 2013; Anderson et al., 2009; Seubert et al., 2013; Ryan et al., 2017; Smith et al., 2018b; Umhau et al., 2018). While we acknowledge that there may be minor impacts in the environment for concentrations below this threshold, use of a common value enables comparison between different studies, regions, and methodologies of DA detection. When testing our statistical approaches across this range, we found no significant changes in the overall results; pDA observations below the 0.05 $\mu g/l$ threshold were set to zero. We calculated monthly probabilities of events and non-events as the number of events or non-events divided by the total number of pDA observations in that month (Table 1 and bars in Fig. 3). Only months with more than four pDA observations were used to calculate event probabilities.

Table 1
Description of the types of datasets generated for this study.

Time series type	Temporal characteristics	Definition
Raw data	N/A	All raw data with minimal processing, setting pDA values below detection to 0. Other outliers removed for variables other than pDA.
Full time series	Daily, weekly, monthly	Includes long-term trends, seasonality, and non-events as zeros.
Anomalies during an event	Daily, weekly, monthly	Removes long-term trends and seasonality and removes non-events.
DA event probabilities	Monthly	Number of events or no-events per month divided by the total number of pDA observations in that month, considering only months with > 4 pDA points.

2.3. Time series analysis

Removing long-term trends and seasonality is key to identifying local variations and drivers of particularly intense DA events. Long-term trends and seasonality were calculated as follows: First, we applied a log10($X + 1$) transformation for pDA, and log10(X) transformation for Chl-a and river flow. For long-term trends, we applied two times a moving mean with a width of two years centered on the specific date. Detrended time series were then calculated by subtracting long-term trends from the original time series. For pDA observations, non-events were kept as zeros. Seasonality was calculated from the annual cycle by fitting spline curves to detrended data sorted by month, using seven nodes to capture low-frequency signals with time-scales greater than approximately two months. Next, we removed the seasonality from the detrended time series to produce the "detrended, deseasonalized anomalies" or just "anomalies" (Supplementary Fig. S1, Table 1). For the calculation of trends in SBC and SPC regions, we removed the period before 2008 because of the scarcity of DA observations before that year.

2.4. Statistical analysis

Correlation analyses (Pearson) on DA drivers (Fig. 2) were conducted using (1) the full time series (which include trend, seasonality, and non-events as zeros) and (2) the time series of anomalies during an event (without trend and seasonality, and with zeros removed) (Table 1). The

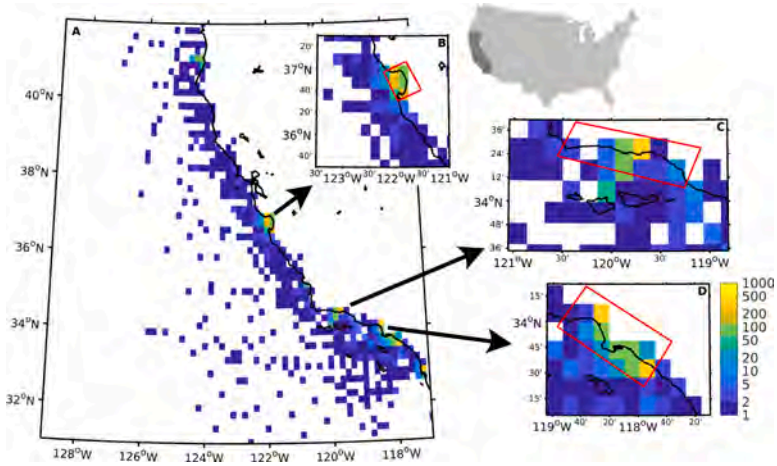

Fig. 1. Number of pDA observation data per grid cell. Colors show the number of pDA measurements in each 20 × 20 km grid box (note the log10-scale). (A) California Coast, (B) Monterey Bay (MB), (C) Santa Barbara Channel (SBC) and (D) San Pedro Channel (SPC). Red boxes show coastal regions from which data were used for time series analyses.

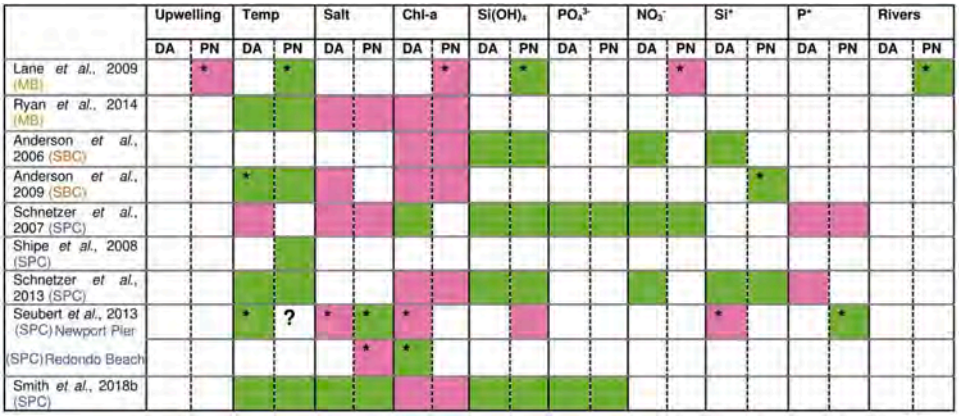

Fig 2. Published correlations between particulate domoic acid concentrations (DA) and *Pseudo-nitzschia* abundances (PN) and environmental variables in the Monterey Bay (MB), Santa Barbara Channel (SBC) and San Pedro Channel (SPC). Environmental variables are indicated in the column headers. Correlative relationships for DA are shown on the left, and for PN on the right of each column. Cells filled in green indicate a negative relationship, and cells filled in pink indicate a positive relationship, as derived from field studies. Asterisks (*) indicate relationships inferred from statistical models. Empty cells indicate that those relationships were not tested, not observed, or not statistically significant. Question marks (?) indicate incongruent or contradictory relationships. Environmental variables consist of: upwelling, Temp = temperature, Salt = salinity, Chl-*a* = chlorophyll-a, $Si(OH)_4$ = silicic acid, PO_4^{3-} = phosphate, NO_3^- = nitrate, Si* = $Si(OH)_4$ - NO_3^-, P* = PO_4^{3-} - NO_3^- / 16, and river influence.

full time series yield a complete picture of correlations, while the anomaly time series highlight relationships during DA events by focusing on anomalous behavior in contrast to more persistent and predictable seasonal cycles and long-term trends. We also calculated correlations between monthly DA event probabilities and environmental variables to evaluate their role on DA outbreaks. Correlations were calculated at multiple temporal lags to detect delayed influences between environmental triggers and pDA concentrations. All correlations discussed in this paper assume a statistical significance level of $\alpha = 0.01$.

To characterize the conditions more conducive to DA outbreaks, we determined their frequency as a function of environmental variables, using full and anomaly daily time series (except for POTW ocean discharge and climate indices, which are monthly). Statistical differences between those distributions were quantified with a non-parametric Kolmogorov–Smirnov test. We defined on-season periods for climate mode analysis using the regional climatology of DA events (Fig. 4), considering months where both probabilities and concentrations are significantly larger than the rest of the year (probabilities above 0.4 for MB and SPC, and above 0.3 for SBC). For conciseness, only Si*, Chl-a, temperature, river flow, and UI are presented in the main text, while the remaining variables are presented in the Supplementary Information.

We further applied a conditional probability analysis to identify environmental thresholds of Chl-a associated with an increased risk of DA events (Sutula et al., 2017). This approach estimates the DA event probability above a particular threshold (a binary variable) given the occurrence of a related, conditional variable. We focused on Chl-a, since it has been positively correlated with pDA concentrations in many previous studies along the California's coast (Fig. 2). The risk was assessed for raw pDA observations above the reference level for DA events (0.05 μg/l). To detect probabilities at the higher end of the distribution, no outliers were removed for Chl-a data. The conditional probability analyses were conducted in R using the *Cprob* package (Allignol et al., 2011) and include confidence intervals based on 1000 iterations of bootstrapped calculations. Inflection points were selected as the first time the 95% confidence interval reached the 0.5 probability of detection of pDA. Above this level, an event was assumed more likely to develop than not. All the statistics discussed in the Results are summarized in Table 2.

Table 2
Description of statistical analysis applied in this study. Variables were grouped in the following four categories: Physics (U.I., MagWind, Temp, Salt); Biogeochemistry (Chl-a, NO_3^-, $Si(OH)_4$, PO_4^{3-}, Si*, P*); Flows (Rivers, POTW); and Climate Modes (NPGO, PDO, MEI). Time series of anomalies were calculated from full time series by subtracting the climatological seasonal cycle and long-term trend.

Time scale	Statistics considered	Full time series	Time series of anomalies (during events, DA>0)
Daily	Correlations up to two lags	Physics, Biogeochemistry, River Flows	Physics, Biogeochemistry, River Flows
Weekly	Correlations up to two lags	Physics, Biogeochemistry, River Flows	Physics, Biogeochemistry, River Flows
Monthly	Correlations up to three lags	All variables	Physics, Biogeochemistry, Flows, Climate Modes (without anomalies)
Monthly	Correlation of pDA probability up to three lags	All variables	
Daily (except POTW)	Frequency of DA events/non-events with K–S test	Physics, Biogeochemistry, Flows	Physics, Biogeochemistry, Flows
Daily	Conditional probability	Chl-a (without outlier removal)	
	Frequency of DA events and no events per month on modes	Climate Modes	

3. Results

In the following sections, we first discuss the correlative relationships from the statistical analysis of pDA and environmental variable time series by region (Sections 3.1–3.3). Next, we discuss results from the statistical analysis of pDA and environmental variable time series by region (Sections 3.1–3.3). Second, we discuss how the risk of DA events increases during phytoplankton blooms in the three regions, by analyzing the conditional probability of DA events as a function of Chl-a concentrations (Section 3.4). Lastly, we detail the impacts of climate variability on PN HABs for the three regions, by analyzing the frequency of DA events and non-events during different climatic phases (Section 3.5).

3.1. Monterey Bay

Interannual variability in pDA is apparent in the MB time series (Fig. 3A), which shows recurrent but highly variable annual maxima. The highest pDA concentrations were observed in June 2015 (63.69 µg/l, Fig. 3A), with seven additional years characterized by high event

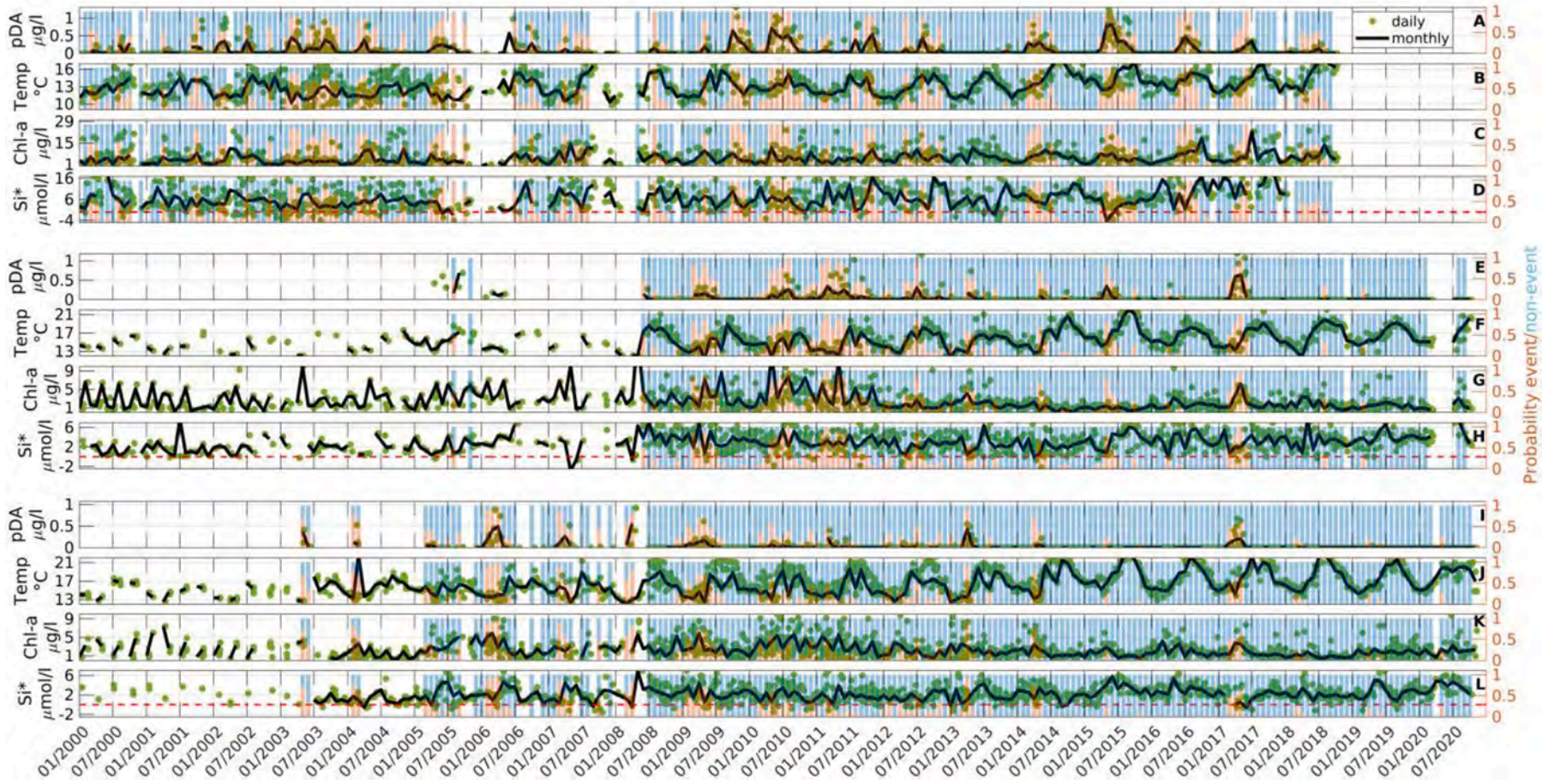

Fig. 3. Time series of chlorophyll (Chl-a), Temperature (Temp), Si* = $Si(OH)_4$ - NO_3^-, and log10(pDA +1). Green dots show daily, spatially gridded time series and solid black lines the monthly time series, with values in the left y-axis. Background colors show the monthly probabilities of events (orange) and non-events (blue) with values on the right y-axis. Horizontal red dash lines show Si* = 0. (A-D) Monterey Bay, (E-H) Santa Barbara Channel, (I-L) San Pedro Channel.

probabilities (2005, 2008, 2009, 2010, 2014, 2016 and 2017, Fig. 3A). Typically, events are most likely between spring and summer, most commonly occurring between April and August (blue bars in Fig. 4A). A secondary period of high event probabilities occurs between October and November, although probability of occurrence is less than in the spring and summer (Fig. 4A). Monthly mean pDA concentrations (orange line in Fig. 4A) reveal similar seasonal cycles as event probabilities, with a narrower peak in spring, and low values in October and November. Important relationships between Chl-a, temperature and nutrients are also observed, with Chl-a concentrations generally peaking in late spring, and temperature and nutrients during late summer and winter-to-spring, respectively (Fig. 3B-D; see Supplementary Fig. S2 for additional variables in MB). pDA concentrations show a positive correlation with wind magnitude and UI, but only for the full time series, potentially reflecting the overarching effect of the seasonal cycle (Fig. 5A and Supplementary Fig. S3). However, pDA concentrations are weakly correlated with wind magnitude over short timescales (2 week or less), and event probabilities do not show significant correlations with UI and wind magnitude (Fig. 6A, and Supplementary Fig. S4). The relationship with upwelling is also reflected in the negative correlations with temperature (only for daily anomaly time series), and positive correlations with salinity (Fig. 5A). Similar to upwelling, the relationship between pDA and Chl-a is robust across timescales and time lags (Fig. 5A).

Negative correlations are observed between pDA and $Si(OH)_4$, PO_4^{3-}, NO_3^- (only weekly), Si*, and P* across timescales (Fig. 5A), with similar patterns for event probabilities (Fig. 6A). We also observe negative correlations between pDA concentrations and rivers flow (Fig. 5A), but no correlation with events probabilities (Fig. 6A). These patterns are supported by the distribution of environmental variables during event and non-events (Fig. 7, upper panels). For example, DA events are more common during upwelling (positive values of UI, Fig. 7A), when waters are anomalously cooler, and saltier (Fig. 7B-C; Supplementary Fig. S5). For Chl-a, we observe a clear threshold at which events become more likely than non-events (> 3.8 $\mu g/l$). Moreover, during events, all nutrients are skewed towards lower values (Supplementary Fig. S5). In particular, the silica deficit (Si*) shows the strongest difference between events and non-events (Fig. 7D), with events occurring more frequently preferentially when Si* drops below 5.7 μmol/l. Finally, events are more frequent during periods of weaker river flow (Fig. 7E).

3.2. Santa Barbara channel

Significant variability in pDA outbreaks is also observed in SBC (Fig. 3E), although with lower concentrations than in MB. The highest pDA concentrations occurred in May 2015 (75.20 µg/l), with three other years with event probabilies of one (2010, 2011 and 2017, Fig. 3E). From a climatological point of view, pDA concentrations and event probabilities peak between March and June (Fig. 4B), with a secondary concentration maximum in late July, and high event probability through the summer. Chl-a and nutrients also reach maxima in spring (Fig. 3G,H, Supplementary Fig. S6), while temperatures peak in early spring to summer (Fig. 3F).

SBC is characterized by systematic positive relationships between pDA and wind-driven upwelling across multiple timescales (Figs. 5B and 6B), corroborated by negative correlations with temperature and positive correlations with salinity and Chl-a (Figs. 5B and 6B). As in MB, we observe negative correlations with $Si(OH)_4$, Si*, and P*, while correlations with NO_3^- and PO_4^{3-} are either non-significant or positive. While major rivers and discharge sites are minimal in SBC, pDA concentrations and event probabilities positively correlate with higher river flow and POTW discharge (Figs. 5B, and 6C).

Similar to MB, DA events are more common during phases of stronger upwelling, cooler temperatures, elevated Chl-a (above a threshold of 2.6 $\mu g/l$), $Si(OH)_4$ and PO_4^{3-} deficits (in particular Si* < 1.8 μmol/l), and higher river flow (Fig. 7F-I; Supplementary Fig. S5). These relationships appear more robust for winds, temperature, Chl-a, and river flow when considering the full time series, and for nutrients and nutrient deficits when considering anomaly time series.

3.3. San Pedro channel

DA events are more sporadic and often weaker in SPC as compared to MB and SBC (Fig. 3I). The highest concentrations occurred in March 2011 (52.30 µg/l) and high event probabilities of ~0.9 were observed in 2006 and 2013. Typically, events are more common between February and May (Fig. 4C), reflecting a shift to an earlier DA season in this southerhnmost region and less common events in summer. This coincides with maximum climatological pDA concentrations in March (Fig. 4C), together with early spring Chl-a, temperature, and nutrient maxima (Fig. 3J-L; Supplementary Fig. S7).

Similar patterns in the correlations for UI, temperature, Chl-a are observed in SPC as compared to other regions, especially SBC (Fig. 5C), supporting an analogous link with upwelling. However, in SPC, pDA concentrations correlate positively with $Si(OH)_4$ and PO_4^{3-} (Figs. 5C, 6C), while the negative correlation with Si* is maintained (Fig. 5C). As in SBC, our results indicated a positive influence of river flow and POTW ocean discharge on pDA concentrations and event frequency (Figs. 5C and 6C).

The number of events and non-events as a function of environmental conditions is consistent with these patterns, with stronger upwelling, cooler temperatures, higher Chl-a concentrations (> 2.6 $\mu g/l$), more intense silicic acid deficit (< 1.8 μmol/l), and higher river flows favoring pDA outbreaks (Fig. 7K-O). Additionally, of the two Southern California

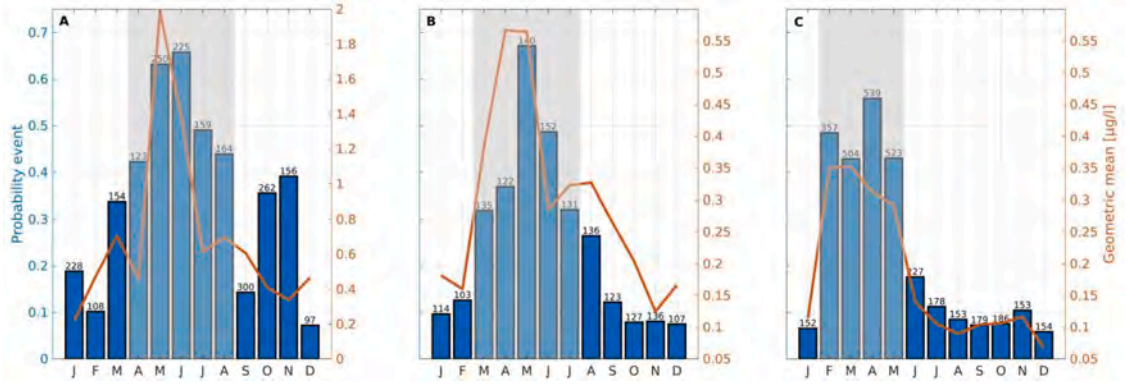

Fig. 4. Histograms of climatological monthly probabilities of pDA events (blue bars, left y-axis) and the climatological monthly geometric mean pDA concentration during events (orange line, right y-axis). Gray shaded boxes show the main season of DA outbreaks. The total number of individual observations for that month is shown on top of each bar. (A) Monterey Bay, (B) Santa Barbara Channel, (C) San Pedro Channel.

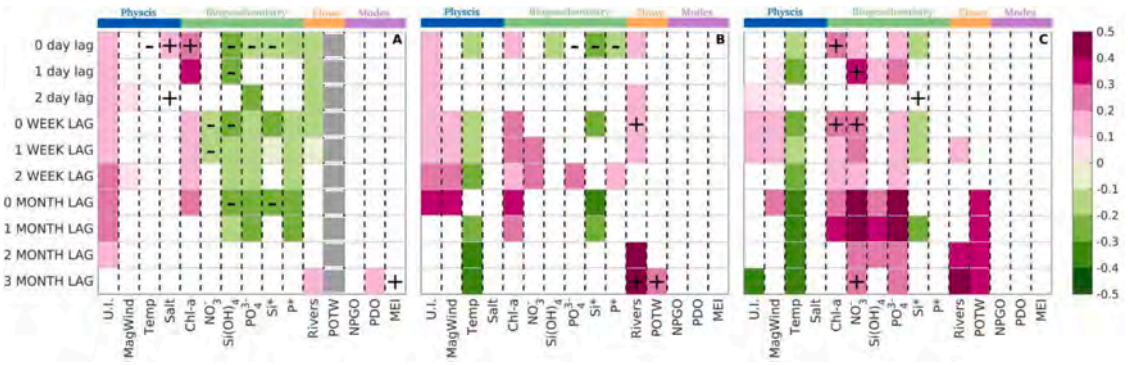

Fig. 5. Correlation matrix of pDA concentration against environmental variables for (A) Monterey Bay, (B) Santa Barbara Channel, and (C), San Pedro Channel. Correlations with daily time series are indicated in lowercase on the y-axis; correlations with weekly or monthly time series in uppercase on the y-axis. Colors indicate correlations for the full time series; +/- symbols indicate correlations for anomaly time series during events. Vertical dashed lines separate different variables, horizontal grey lines separate different temporal lags. Gray rectangles indicate lack of data. All correlations are significant at $\alpha = 0.01$. The variables shown on the x-axis are: Upwelling Index (U.I.), Wind Magnitude (MagWind), Temperature (Temp), Salinity (Salt), Chlorophyll-a (Chl-a), nitrate (NO_3^-), silicic acid ($Si(OH)_4$ -), phosphate (PO_4^{3-}), silicic acid deficit relative to nitrate ($Si^* = Si(OH)_4 - NO_3^-$), phosphate deficit relative to nitrate ($P^* = PO_4^{3-} - NO_3^- / 16$), flow from rivers, flow from POTW, North Pacific Gyre Oscillation index (NPGO), Pacific Decadal Oscillation index (PDO), and Multivariate El Niño-Southern Oscillation Index (MEI).

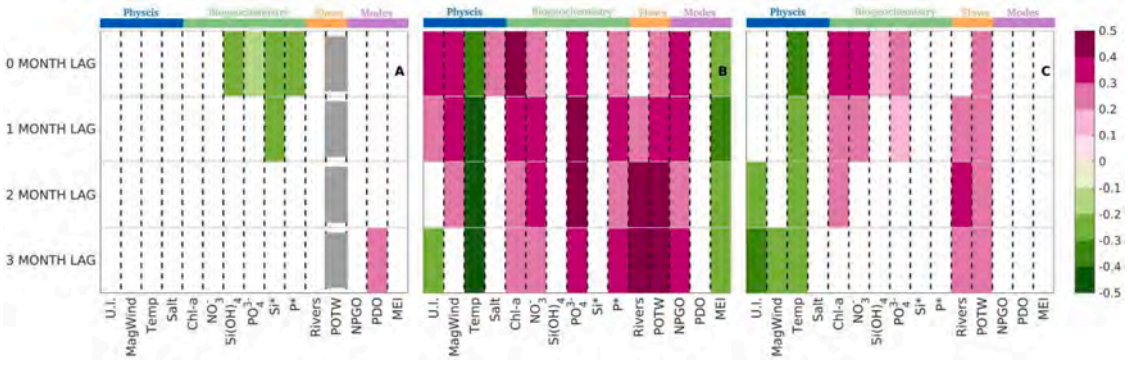

Fig. 6. Correlation matrix of pDA event probability against environmental variables for (A) Monterey Bay, (B) Santa Barbara Channel, and (C) San Pedro Channel. Vertical dashed lines separate different variables, horizontal gray lines separate different temporal lags. All correlations are significant at $\alpha = 0.01$.

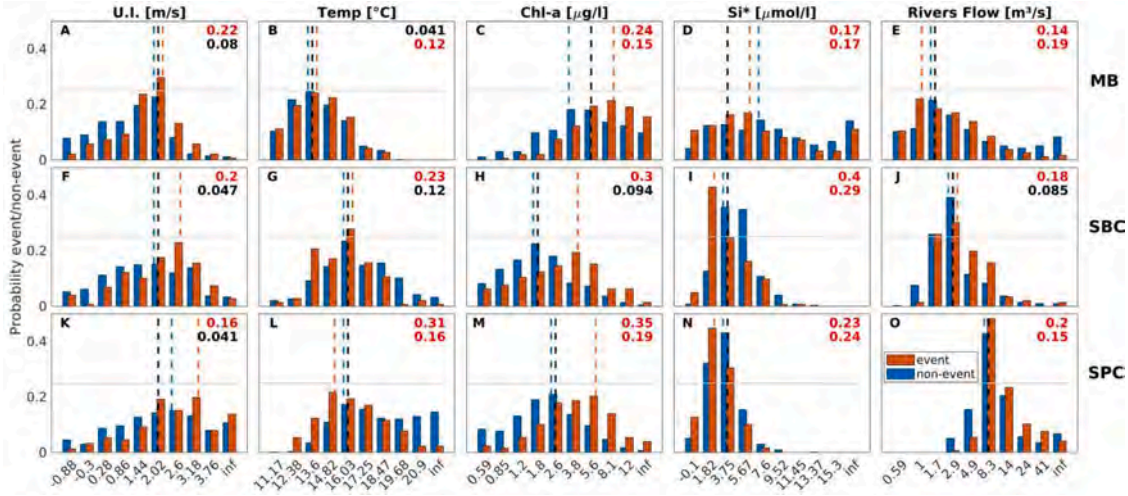

Fig. 7. Probabilities of events (orange) and non-events (blue) as a function of environmental variables. For each variable, counts of observations during pDA events and non-events are binned in 10 equally spaced bins between the 5% and 95% percentiles of that variable. Numbers in each panel show results of a KS-test assessing whether events and non-events follow the same distribution. Higher numbers indicate increasingly different distributions. Top numbers refer to a test using full time series, and bottom numbers to anomaly time series. Red numbers show significance at $\alpha = 0.01$. Vertical dashed lines show the mode of the distribution for events (orange), non-events (blue), and for all measurements (black). Horizontal gray lines show probability of 0.25. The x-axis shows the upper-bound of each interval.

areas examined, SPC is the only one where events during higher POTW ocean discharge are statistically different from non-events (Supplementary Fig. S5).

3.4. Increased risk of DA events during Chl-a blooms

Based on a conditional probability analysis, baseline probabilities of pDA > 0.05 $\mu g/l$ (our definition of an event) regardless of the value of Chl-a are 0.38, 0.34 and 0.32 for MB, SBC, and SPC respectively (Fig. 8). In other words, pDA is likely to be above the detection limit 32–38% of the time, making the presence of pDA a pervasive feature. The 95% confidence interval intersects the value of 0.5 for the probability of an event (pDA > 0.05 $\mu g/l$) at Chl-a concentrations of 5.4, 1.8, 3.3 $\mu g/l$ in MB, SBC and SPC respectively (stars in Fig. 8). Those are the concentrations of Chl-a at which an event is more likely to be observed than not. The slopes of the conditional probabilities in both south coast subregions are steep, with a doubling in pDA detection probability over the Chl-a range of 1–5 $\mu g/l$ in SBC, and 1–10 $\mu g/l$ in SPC. In SBC, a further inflection point of accelerated risk is apparent at 12 $\mu g/l$.

3.5. Impacts of climate variability on DA events

Limited relationships were found between climate fluctuations, pDA concentrations, and the frequency of outbreaks (Figs. 5 and 6). Notable relationships in MB are a weak positive correlation between pDA concentration, PDO (full time series), and MEI (anomaly time series) (Fig 5A), and a positive correlation between the probability of an event and PDO (Fig. 6A), all at three-month lags. In SBC, we found a systematic negative correlation between event probability and MEI, particularly strong at a one-month lag, while always positive for NPGO (Fig. 6B). The lack of significant correlations in other regions may be related to the limited duration of the time series, which are likely too short to robustly detect relationships with climate phases that vary over decades.

To further investigate the role of climate variability, we quantified the probability of DA events and non-events during positive and negative climate phases (Fig. 9). In general, events are less frequent than non-events, and are more common during the on-season period (gray boxes in Fig. 9). In contrast, non-events are more common off-season. Across all regions, DA events occur during both positive and negative phases of the climate indices (Fig. 9), with a degree of regional specificity (see Supplementary Table S3 for the number of events and non-events by region and climate phase).

In MB, events are more likely to occur on-season during negative NPGO phases and positive PDO and MEI phases, with a nearly opposite pattern for non-events off-season (Fig. 9A-C). The picture is different in SBC and SPC, which share similar characteristics in their response to climate variations. In both regions, events are more common on-season during negative phases of the PDO and MEI, while they are somewhat more common during positive NPGO in SBC, and negative NPGO in SPC (Fig. 9D-I). In contrast, non-events are more common in both regions off-season, during positive NPGO and negative PDO and MEI phases.

4. Discussion

4.1. Similarities across California coastal regions

Regardless of the regional specificities in timing and intensity of upwelling along the California coast, pDA outbreaks are strongly associated with upwelling coastwise (Fig. 10). This is reflected by positive correlations with the Upwelling Index (UI) across daily to monthly timescales (Figs. 5 and 6) and increasing event frequencies under more vigorous upwelling (Fig. 7A, F, K). Consistently, Schnetzer et al. (2013) found a strong link between upwelling in SPC along the Los Angeles coast and highly toxic *P. australis* events. Seubert et al. (2013) reported similar findings, in addition to large size-class PN cell abundances (often associated with significant DA production). Upwelling was also included as a powerful predictor in the PN model for MB by Lane et al. (2009), and Anderson et al. (2009) demonstrated significant association between pDA and upwelling in SBC.

Nonetheless, the relationship with upwelling appears nuanced. For example, findings from a sediment trap time series suggest that while *P. australis* blooms and DA events are more frequent during upwelling, they also occur during relaxation phases (Sekula-Wood et al., 2011). In our analysis, the relationship between pDA and upwelling is only significant when considering full time series, but not when considering anomaly time series (Fig. 5A, B, C). That is, anomalously strong upwelling does not appear more likely to support high pDA concentrations than climatological upwelling variability. Seegers et al. (2015) suggested that it is not only the occurrence of upwelling, but its duration, intensity, frequency, the composition and physiology of extant PN populations, and subsequent stratification that can also drive an event and/or push it offshore. Together with the relatively uniform distributions of UI during events (Fig. 7A, F, K), our results suggest a window of opportunity where DA outbreaks are more likely to occur, especially considering the ubiquitous occurrence of DA (probability greater than 0.3 for pDA event, Fig. 8; Umhau et al., 2018), while other factors contribute to their overall intensity. It should also be noted that, especially in the central Coast (where MB is located), Chl-a blooms lag strong upwelling, and generally take place when the water column re-stratifies. This may reduce correlations between variables that are tied to the progression of upwelling.

Events are also positively associated with high Chl-a across all regions, suggesting a coastwide link between phytoplankton blooms, increased PN abundance, and DA outbreaks. Positive relationships between DA and Chl-a have been observed in several previous studies (Fig. 2). A relationship between these parameters seems obvious, as a significant DA event would be unlikely in the absence of a substantial bloom (although high Chl-a does not necessarily mean that a DA event will occur). In other words, PN blooms are often a feature of springtime diatom blooms in California waters.

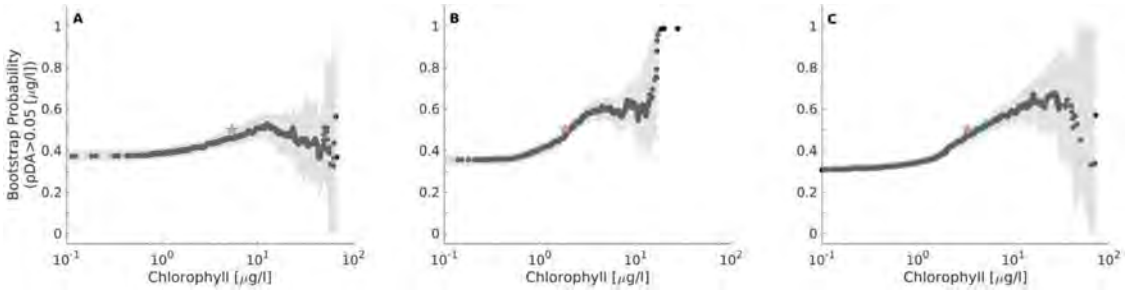

Fig. 8. Probability of a pDA exceeding detection level of 0.05 $\mu g/l$ for specific Chl-a concentrations for (A) Monterey Bay, (B) Santa Barbara Channel, and (C) San Pedro Channel. grey shadings show the 95% confidence intervals of bootstrap values (1000 iterations). Red stars indicate the first time the 95% confidence intervals reach the 50% probability of pDA detection.

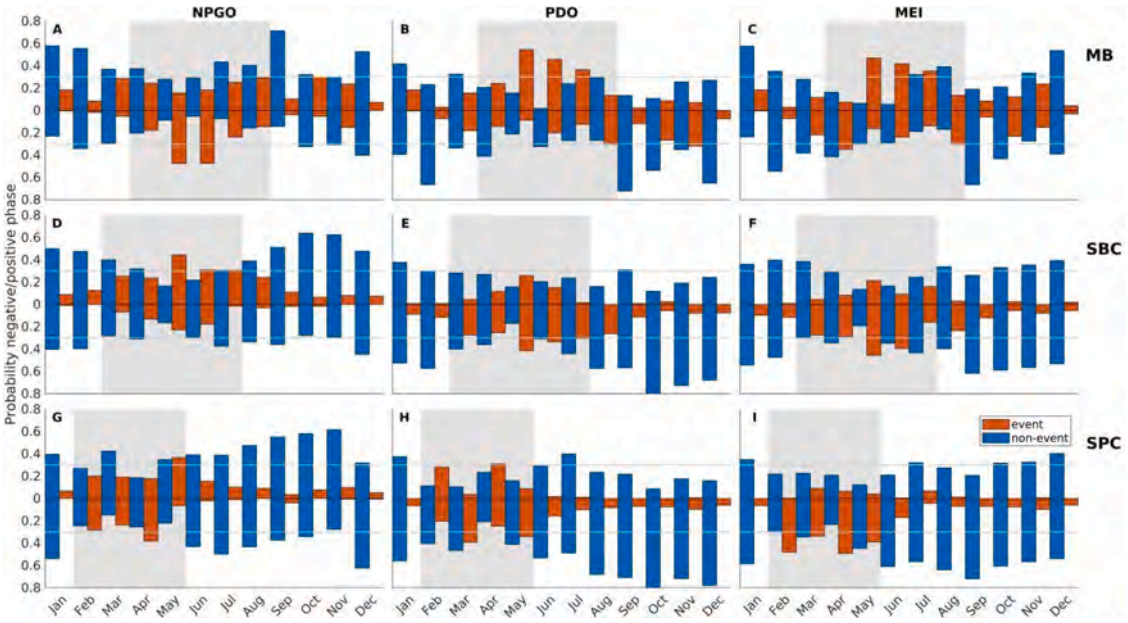

Fig. 9. Probabilities of pDA events (orange) and no events (blue) during different phases of North Pacific Gyre Oscillation index (NPGO), Pacific Decadal Oscillation index (PDO), and Multivariate El Niño-Southern Oscillation Index (MEI). Values above zero indicate positive indices, below zero negative indices. In each panel, the shaded boxes show the on-season period; horizontal gray lines indicate probabilities above 0.3. For each month, the sum of the probability for events and non events under positive and negative phases is equal to 1 by construction.

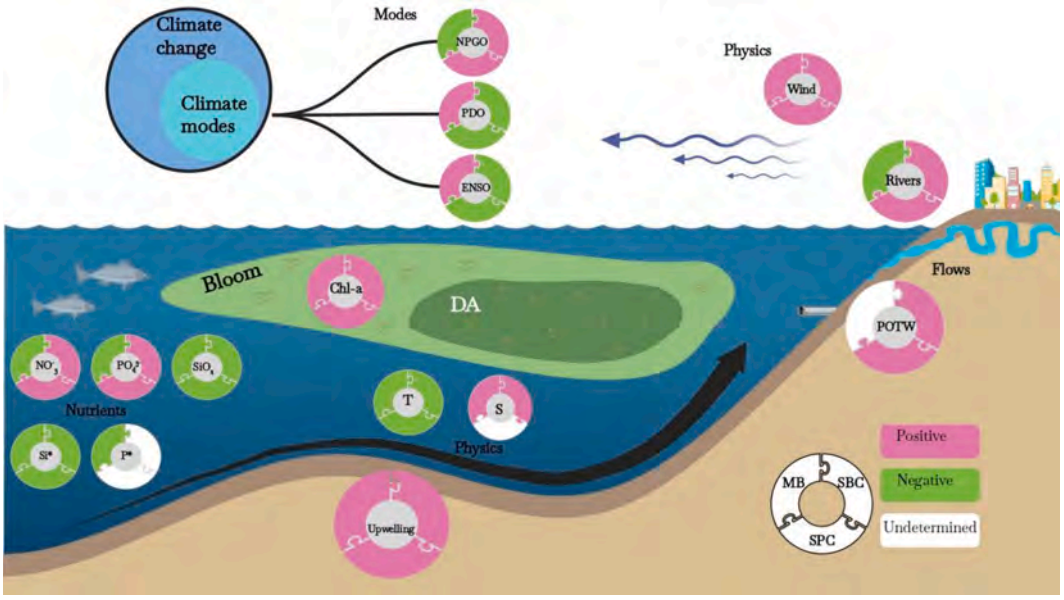

Fig. 10. Schematic of the role of environmental factors in Domoic Acid (DA) production in the different regions tested in this study.

While the relationship between DA events and Chl-a is not a causative one, it is a useful risk metric for the prediction and potential management of these events. Chl-a has been utilized to assess eutrophication levels in other systems (Bricker et al., 2003; 2008; Zaldivar *et al.*, 2008; Devlin et al., 2011; Harding et al., 2014; Sutula et al., 2017), and bulk phytoplankton biomass endpoints intended to avoid risk of toxic HABs are often integrated into nutrient or eutrophication water quality criteria (Harding et al., 2014; Sutula et al., 2021) and other HAB mitigation efforts (Sutula and Senn, 2017). Chl-a has also been employed as a positive predictor in several subregional models of toxigenic PN blooms (Lane et al., 2009; Seubert et al., 2013).

Analysis of event probabilities indicates that the likelihood of DA events increases at higher Chl-a concentrations (Fig. 7C, H, M; Fig. 8), and pDA is likely to be above 0.05 $\mu g/l$ between 31 and 38% of the time across all regions (Fig. 8). These values correspond well with the value of ~35% for DA exceeding the alert level (75 ng DA g^{-1}) in San Francisco Bay reported by Sutula et al. (2017). Furthermore, the conditional probability of DA events reaches a baseline value of 50% at ~5 $\mu g/l$ Chl-a in MB and ~1–3 $\mu g/l$ Chl-a in the southern regions (Fig. 8), with an additional notable inflection point of increased DA event risk in SBC at ~12 $\mu g/l$ Chl-a (Fig. 8B, C). These are useful reference points to guide monitoring programs and support predictive modeling efforts.

There are also instances of elevated Chl-a observations that are not associated with DA events, suggesting dominance of non-DA producing taxa. Indeed, cell counts of large size-class PN cells have been identified as a more reliable predictor of DA events than Chl-a in SPC (Seubert

et al., 2013). Although PN cell abundance could yield a much tighter relationship with DA events, these observations are often rare relative to Chl-a. PN cell abundance is also an imperfect predictor of pDA concentration because toxin production depends on the PN species in a bloom and their physiological state, which are not easily resolved by microscopy, and thus rarely characterized (Bowers et al., 2018; Umhau et al., 2018; Smith et al., 2018b).

Modeling studies for the Southern California Current show that anthropogenic nutrient inputs in regions with significant agricultural activities or dense coastal population can greatly amplify net primary productivity (*e.g.*, in the Bight, Kessouri et al., 2021a). However, consistent, direct statistical associations between pDA and either riverine inputs or POTW discharges to ocean outfalls have been more difficult to establish. In MB, we observed negative correlations and less frequent DA events during high river discharge (Figs. 5A, and 6E; Fig. 10), consistent with previous studies (Trainer et al., 2000; Kudela *et al.*, 2003; Jester et al., 2009; Lane et al., 2009). Positive correlations between DA events and high river flows were found in SPC and SBC (Fig. 7B, C). No statistically significant difference was found between variations in local POTW discharge volume and DA events/non-events in SBC (Supplementary Fig. S5) despite the positive correlations with magnitude and event probability (Figs. 5B, 6B). In SPC, however, we found positive correlations with POTW outfall discharge (Figs. 5C, 6C) and statistically significant differences between DA events and non-events with different values of the discharge (Supplementary Fig. S5).

Multiple reasons exist for these conflicting statistical associations, both within and between regions. (1) Freshwater inputs and seasonally varying nutrient ratios could either favor PN or favor other phytoplankton species that outcompete them (Ryan et al., 2014). (2) Relying on riverine discharge rather than riverine nutrient load data could confound the analysis, because peak flows can either coincide with increased nutrient loads or dilute them (Schnetzer et al., 2007; 2013). (3) Levels of POTW nutrient removal vary along the coast, so outfall discharge volume alone does not always encapsulate the strength of nutrient loading, and distal terrestrial sources can be more significant drivers of PN HABs than local ones (Kessouri et al., 2021a). (4) The strength of significant correlations could depend on the ocean state (well mixed *vs.* stratified; Kessouri et al., 2021a) and the timing of upwelling relative to terrestrial inputs, which could inhibit toxigenic blooms via out-competition (Schnetzer et al., 2013), or create a seasonal additive effect that makes it difficult to untangle their relative signals (Sekula--Wood et al., 2011; Smith et al., 2018a). (5) A spatial or temporal decoupling of terrestrial inputs and pDA events may occur, depending on residence time and a host of other intrinsic factors. For example, one possible explanation for the delayed correlation with rivers at 2 to 3 months lag (Figs. 5C, 6C) in SPC could be the persistence of a PN community in thin layers as "seed populations" prior to an event (Seegers et al., 2015). In particular, the resuspension of seed populations and "cryptic blooms" in subsurface Chl-a maxima and thin layers (McManus et al., 2008) are potentially significant drivers of nearshore toxic blooms (Rines et al., 2010; Timmerman et al., 2014; Ryan et al., 2014; Seegers et al., 2015; Umhau et al., 2018). As with MB and SBC, modeling studies are needed to parse the relative importance of point source and nonpoint sources of nutrients from ocean discharges and rivers in these regions, relative to other factors.

Physiological state has been repeatedly reported as a factor in DA production by PN, and indeed Si and P limitations have been associated with increased DA production in field and laboratory studies (Fig. 2; Lelong et al., 2012; Moreno et al., 2022). Conversely, sufficient nitrogen is required for DA synthesis (Pan et al., 1998), although DA production under nitrogen limitation has been documented (Kudela et al., 2002). Accordingly, decreased $Si(OH)_4$, Si*, and P*, and increased NO_3^- concentrations have been included in models for abundance of PN in MB (Lane et al., 2009), SBC (Anderson et al., 2009) and SPC (Seubert et al., 2013). These results align with our findings of negative correlations between events and $Si(OH)_4$, PO_4^{3-}, Si* and P* across multiple timescales in MB and SBC (Figs. 5A, B; 10). Across regions, lower values of Si* (Fig. 7D, I, N), $Si(OH)_4$, PO_4^{3-} and other nutrient ratios (Supplementary Fig. S5) are associated with a greater probability of events against non-events.

4.2. Regional differences

4.2.1. Monterey Bay

Negative correlations between pDA and $Si(OH)_4$, PO_4^{3-}, NO_3^- Si*, or P* (Fig. 5A) suggest that pDA accumulation in MB most likely occurs under two scenarios. The first scenario is when nutrients are depleted by phytoplankton uptake, but the temperature and salinity signature of upwelling persist (Anderson et al., 2009 in SBC). This nutrient depletion can be intensified when a bloom is trapped in retentive circulation patterns that increase residence time and nutrient drawdown by the entrapped phytoplankton community (Ryan et al., 2014; Anderson et al., 2006).

A second scenario is one where anomalously low nutrient are persistent due to large-scale shifts in oceanic conditions (*e.g.*, climate modes; Ryan et al., 2017). We observed negative relationships between DA events and nutrients from daily to monthly timescales, which suggest a preconditioning of the system to anomalously low nutrients (Figs. 6A and 7A; Trainer et al., 2020a). Anomalous circulation, warm and fresh waters, and/or low nutrient concentrations are associated with positive PDO and MEI phases (Fig. 6A; Mantua and Hare, 2002; Mantua et al., 1997; Jacox et al., 2015), and increase the likelihood of events on-season (Fig. 9B, C). Indeed, the massive 2015 DA outbreak along the U.S. West Coast is thought to be a consequence of faster growth and/or Si limitation response after the establishment of an anomalously warm water mass (Du et al., 2016; Ryan et al., 2017), likely related to positive phases of PDO and ENSO (McCabe et al., 2016; McKibben et al., 2017). Our results agree with that hypothesis (Fig. 10), with weak but positive relationships between pDA concentration and event probabilities with PDO and MEI (Figs. 4A, 6A). Accordingly, we observed more frequent events during negative NPGO and positive PDO and MEI (Fig. 9A, B, C). Although their observations were north of our domain, McKibben et al. (2017) also found positive correlations between DA concentrations in razor clams and warm phases of both PDO and ENSO. In our analysis, we found a negative rather than positive correlation between pDA anomalies and temperature anomalies, and positive correlations with salinity and Chl-a (Fig. 5A). This suggests that seasonal upwelling may reduce the effects of climate shifts locally (warm to cold water), but anomalously low nutrients (here both $Si(OH)_4$ and PO_4^{3-} relative to NO_3^-; Du et al., 2016; Ryan et al., 2017; McManus et al., 2021) may be maintained due to weaker upwelling and a deeper nutricline during these climate phases (Kudela *et al.*, 2003; Ryan et al., 2017).

4.2.2. Santa Barbara channel

Upwelling plays an important role for DA events in SBC, although with some key distinctions. The persistent negative correlation with Si* across multiple lags indicates an association with Si limitation when NO_3^- is replete (Fig. 5B). This finding implicates upwelling, but without the same dependence on anomalously low nutrients as in MB (Fig. 10). This is likely because of excess $Si(OH)_4$ drawdown during PN blooms (Anderson et al., 2009), reinforcing the hypothesis that nutrient stress is a major trigger for DA production, with NO_3^- being necessary for biosynthesis. Anderson et al. (2009) suggested that the negative relationship with $Si(OH)_4$, despite the positive correlation with upwelling, derives from a period of upwelling relaxation, where the signal of upwelling is still present, but nutrient availability (specifically $Si(OH)_4$) has diminished, presenting a competitive window of opportunity for PN. DA outbreaks under these conditions are not explicitly linked to upwelling events, but with upwelling relaxation or late phases in the succession of phytoplankton (Sekula-Wood et al., 2011; Umhau et al., 2018). However, as in MB, outbreaks do not occur each upwelling

season, suggesting that other factors also contribute.

Our analysis is consistent with the idea that a specific "temperature envelope" supports toxigenic species, as hypothesized by Smith et al. (2018a), who showed that pDA in the Bight was always associated with temperatures below 21 °C (Fig. 7G). Barron et al. (2010), reported changes in SBC ecosystem after the year 2000–2001 that led to the dominance of more cold-adapted species. A cold-water signal could be maintained and accompanied by enhanced nutrient supply, phytoplankton blooms, and pDA accumulation when climate modes promote more intense upwelling (-PDO, +NPGO, -MEI; Figs. 6B, 8D-F; Barron et al., 2013), especially on-season, consistent with sediment trap observations (Sekula-Wood et al., 2011). Positive correlations between events and nutrient concentrations with one to three months lag corroborate this preconditioning of the system (Fig. 6B). From there, retentive features could sustain blooms for longer periods, resulting in nutrient drawdown and eventual limitation (Kudela *et al.*, 2003; Anderson et al., 2006; 2009; Umhau et al., 2018; Smith et al., 2018b). One of the most significant circulation features in this region is a cyclonic eddy that could enhance DA production by favoring retention and nutrient limitation following blooms (Anderson et al., 2006). Another source of upwelled waters to SBC is advection from north of Point Conception (Anderson et al., 2009). Because of the main west-to-east orientation of the coast, climate patterns that promote strong upwelling in SBC may not have a strong local signature, but rather one further north. Periods of relaxation may allow upwelled waters to enter SBC from the north, where they could be trapped within the cyclonic circulation, especially during late summer and fall (Catlett et al., 2021).

4.2.3. San Pedro channel

The specific factors leading to pDA production in SPC are more difficult to interpret compared to other regions. SPC is characterized by higher variability in events frequency and characteristics (Schnetzer et al., 2013; Smith et al., 2018b). For instance, although pDA is detected more than 16% of the time, events are much less frequent than non-events (Fig. 3I).

Positive correlations of pDA with wind, nutrients, and negative correlations with temperature, support a causal relationship with upwelling (Fig. 5C). Higher pDA concentrations during periods of Si deficit (*i.e.*, negative correlation with Si*) indicate that Si limitation may be a primary factor for DA outbreaks in this region, similar to SBC. This is supported by the excess of events relative to non-events at lower Si* and temperature, higher Chl-a, and more intense UI compared to non-events (Fig. 7K-N), in agreement with previous work (Schnetzer et al., 2007; 2013; Shipe et al., 2008; Seubert et al., 2013). Notably, SPC is the only region with a strong temperature difference between events and non-events, which also appears when considering temperature anomalies, and a clear increase in the frequency of events at temperatures below 17 °C (Fig. 7L).

Consistently, events are associated with cooler climate phases and are more common during positive phases of NPGO and negative phases of PDO and MEI (Fig. 9G-I). These climatic conditions reflect stronger upwelling, cooler waters, and increased mixing and nutrient supply (Fig. 10). Additionally, SPC is prone to retention of phytoplankton blooms within small-scale eddies (DiGiacomo and Holt, 2001; Schnetzer et al., 2013) and southward advection from SBC (Catlett et al., 2021). These processes may be key to the development of DA events when other conditions are met.

4.3. Caveats and future work

While our study is based on the most comprehensive pDA compilation to date for the California Coast, the dataset contains a high number of observations below detection. This excess is the result of (1) true zeros that reflect absence of pDA at the time of sampling (structural zeros); and (2) zeros that reflect variable detection limits in the different approaches used to measure pDA over time (sampling zeros) (Wang et al., 2018). We addressed the second cause by setting a common threshold (0.05 $\mu g/l$). This approach inflates the number of sampling zeros in our dataset, increasing overdispersion of the data, and potentially reducing the strength of our statistical analysis (Zuurt *et al.*, 2009). However, retaining zeros is essential to capturing the dynamic range in the system. We ameliorated this issue by analyzing different types of time series (full and anomaly) and monthly probabilities. A standard methodology for sampling DA and defining events based on pDA levels of concern, and not only on toxin content in animal tissues, would be beneficial for analysis of causality and modeling consistency. At the same time, surveys and models should account for the partitioning of DA into particulate and dissolved phases, as the latter can identify toxic events when particle aggregation is not favorable, and further help identify triggering factors and ecosystem effects (Umhau et al., 2018).

An additional challenge is low-frequency (*i.e.*, multi-decadal) climate variability that makes the definition of "normal" conditions questionable (Dale et al., 2006; Trainer et al., 2020a). Since DA production was linked to PN just over 30 years ago in 1987 (Bates et al., 1989), time series observations of the toxin are still short relative to the multi-decadal timescale needed to assess the influence of these factors (Dale et al., 2006). Although we observe climate mode signals in our >18-year long time series, climate indices are still not skillful predictors individually, and in some cases, non-events are equally likely during the same climate phases as events (*e.g.*, NPGO for SPC, Fig. 9G). Trends in these variables, as with any other environmental variable, should be taken as an index of enhanced probability (Fig. 10) rather than factors with strong predictive capacity (Wells et al., 2020).

The low number of significant correlations with anomaly time series likely indicates a strong seasonal component to DA events, where anomalous individual environmental variables only contribute to bloom formation in conjunction with recurring seasonal and local physicochemical features. Many of the most comprehensive sampling efforts were conducted during the main season of DA outbreaks, and are therefore poorly representative of annual variability, while also adding seasonal biases and creating gaps in time series (Fig. 3). Notably, a series of routine, long-term monitoring time series exist at fixed locations along the California coast, including the weekly pier monitoring program Cal-HABMAP and the P&B cruises in SBC. However, routine nearshore time series can fail to capture events that only occur away from the coast, or that have stronger relationships with environmental variables offshore. Future research studies and funding opportunities should target additional offshore and "off-season" observations to provide information about the conditions that do not support DA events, and factors that precondition the system and may lead to subsequent DA outbreaks (Wells et al., 2020). In parallel, statistical models should also consider periods of high and low event probabilities (Lane et al., 2009; Anderson et al., 2016). This would enable more robust statistical analyses, and, in the long run, improve understanding of the role of decadal variability and long-term climatic trends.

Limitations related to the type of data collected still hinder mechanistic analyses. Only pDA samples, without any other environmental correlates, were collected in many of the studies populating the early years of our time series. We addressed missing environmental correlates by combining environmental observations from other programs and matching the approximate location and time. When possible, future studies should collect a baseline suite of environmental variables, together with pDA, including salinity, temperature, macronutrients, and Chl-a. Furthermore, some explanatory factors are rare or completely missing from our data set, even though previous studies have demonstrated their importance (*e.g.*, pCO_2, different nitrogen forms, light intensity, grazing, bacterial community, trace metals, and PN species and abundance; see Wingert and Cochlan, 2021; Radan and Cochlan, 2018; Thorel et al., 2014; Lundholm et al., 2018; Sison-Mangus et al., 2014; Wells et al., 2005; Trainer et al., 2012; Smith et al., 2018b). The potential influence of riverine and wastewater inputs also remains poorly

understood (this study; Wells et al., 2020).

Work should also focus on the lag-perspective of DA outbreaks (*i.e.*, analysis of the conditions before, during, and after an event; Wells et al., 2020). The succession of phytoplankton species is a key aspect in HAB-related problems (Chai et al., 2020), especially in the context of variable ocean conditions as upwelling weakens (Chavez et al., 2017). Monitoring of PN and other species could help elucidate key risk factors (Catlett et al., 2021). For instance, a time series of environmental DNA data in MB between 2008 and 2020 (Chavez et al., 2021) suggests that DA events correlate more strongly with the abundance of *P. australis* relative to other PN groups (compare Fig. 3 here with Fig. 13 in Chavez et al., 2021). The ongoing growth of environmental DNA studies is likely to shed light on the role of species succession and competition and the dynamics of DA events.

4.4. Consistency with PN HABs beyond California waters

The conditions described in this study are not unique to California waters. PN species often bloom in upwelling regions, explaining a research focus on eastern boundary upwelling systems with characteristics similar to the California Current (Trainer et al., 2008; Lelong et al., 2012). DA outbreaks have been linked to upwelling at a variety of sites, including along the French coast (Husson et al., 2016), the Benguela upwelling (Gai et al., 2018; Pitcher et al., 2020), the Atlantic coast of the Iberian Peninsula (Velo-Suarez *et al.*, 2008; Palma et al., 2010), the Mozambique Channel (Kelchner et al., 2021), and the southern Gulf of California (Gárate-Lizárraga et al., 2007; García-Mendoza et al., 2009).

Similar relationships between DA and temperature, salinity, Chl-a, silicic acid, Si*, P*, and nitrate as found in this study have been documented in a variety of coastal settings. These include North American waters, such as Prince Edward Island (Subba Rao *et al.* 1988; Smith et al., 1990), the Gulf of Maine (Clark et al., 2019), Chesapeake Bay and South Carolina (Van Meerssche and Pinckney, 2017), and the Gulf of Mexico (Dortch et al., 1997; Doucette et al., 2008; Macintyre et al., 2011; Liefer et al., 2013; Bargu et al., 2016); European waters, such as the North Sea (Delegrange et al., 2018), the French Atlantic and English Channel (Husson et al., 2016; Thorel et al., 2017), and the Mediterranean Sea (Ujević *et al.* 2010; Arapov et al., 2020; Kvrgić et al., 2022, Garali et al., 2020); and other global sites ranging from western Japan (Kotaki et al., 1999), to Atlantic Patagonia (Hoffmeyer et al., 2020), Indonesia (Likumahua et al., 2019) and the Caribbean Sea (Córdoba-Mena et al., 2020).

At a small number of sites, a negative relationship between DA and phosphate comparable to our findings in MB has been documented, including the Gulf of Maine (Clark et al., 2019), Gulf of Mexico (Liefer et al., 2013), and the French Atlantic, and the Southwest Mediterranean Sea (Husson et al., 2016; Garali et al., 2020). In contrast, positive relationship with phosphate, comparable to our findings in the Bight, have been observed in South Carolina (Meerssche and Pinckney, 2017).

Riverine inputs have been suggested to stimulate toxic *Pseudo-nitzschia* blooms at a variety of locations (Smith et al., 1990; Horner and Postel, 1993; Zou et al., 1993; Qi et al., 1994; Dortch et al., 1997; Trainer et al., 1998; Scholin et al., 2000; Spatharis et al., 2007; Kudela et al., 2008; Trainer et al., 2009; Bargu et al., 2016; Husson et al., 2016; Córdoba-Mena et al., 2020). Finally, relationships with major climate modes have only been documented along the U.S. North Pacific Coast in Oregon and Washington (Horner and Postel 1993; Taylor and Horner 1994; McCabe et al., 2016; McKibben et al., 2017) as well as Central California (Trainer et al., 2000, 2020b). These sites show correlations between DA and positive El Niño phases that are similar to our findings in MB.

5. Conclusions

With the help of the longest time series of pDA available for California (nearly 20-years), we were able to do a cross-site comparison among DA hotspots with sufficient statistical robustness. By analyzing an extensive set of environmental variables and applying a consistent methodology, we highlight key regional and subregional drivers of DA HABs along the California coast, and factors that should be considered for future model development. For instance, stronger correlations observed in full time series rather than anomaly time series suggest easier predictability linked to the seasonal cycle and broad-scale oceanographic features. At the same time, our analysis indicates a significant predictability role for two relatively simple easy targets in HAB studies: bloom strength (*e.g.*, Chl-a) and nutrient concentrations (specifically, Si limitation). Climate modes could enhance seasonal predictability, albeit with regional specificities that should continue to be investigated as time series increase in length. Finally, we uncover correlations with POTW outfall discharge and river flow that have implications for management, especially in highly urbanized regions of the Southern California Bight. These empirical relationships, which are likely to apply to a variety of coastal settings beyond California waters, improve our understanding of the ecology of PN species and DA events, their relationship with physical, biological, and chemical factors, and the evolution of typical events. This in turn provides context for the development of new model capabilities, and for future short- and long-term prediction of DA outbreaks.

Author disclaimer

All authors have approved the final article.

Declaration of Competing Interest

The authors declare that they have no known competing financial interests or personal relationships that could have influenced the work reported in this paper.

Data availability

Data will be made available on request.

Acknowledgements

This research was supported by the NOAA under Ecosystem and Harmful Algal Bloom (ECOHAB) Award NA18NOS4780174 and NA19NOS4780181. This is ECOHAB publication #1039. This work used the Expanse system at the San Diego Supercomputer Center through allocation TG-OCE170017 from the Advanced Cyber infrastructure Coordination Ecosystem: Services and Support (ACCESS) program, which is supported by National Science Foundation grants 2138259, 2138286, 2138307, 2137603, and 2138296. Additional computational resources were provided by the Hoffman2 computer cluster at the University of California Los Angeles, Institute for Digital Research and Education (IDRE). Data collected in Monterey Bay were supported by the David and Lucile Packard Foundation, and NASA grant 80NSSC21M0032. HABMAP data is supported by SCCOOS and CeNCOOS. M.S.-B. is supported by grants from Becas Chile, ANID. Anonymous reviewers are also acknowledged for their valuable comments on the submitted version.

Supplementary materials

Supplementary material associated with this article can be found, in the online version, at doi:10.1016/j.hal.2023.102435.

References

Allignol, A., Latouche, A., Yan, J., Fine, J.P., 2011. A regression model for the conditional probability of a competing event: application to monoclonal gammopathy of unknown significance. J. R. Stat. Soc. Ser. C Appl. Stat. 60 (1), 135–142.

Anderson, C.R., Brzezinski, M.A., Washburn, L., Kudela, R., 2006. Circulation and environmental conditions during a toxigenic *Pseudo-nitzschia australis* bloom in the Santa Barbara Channel, California. Mar. Ecol. Prog. Ser. 327, 119–133.
Anderson, C.R., Siegel, D.A., Brzezinski, M.A., Guillocheau, N., 2008. Controls on temporal patterns in phytoplankton community structure in the Santa Barbara channel. California. J. Geophys. Res. Oceans 113 (4).
Anderson, C.R., Siegel, D.A., Kudela, R.M., Brzezinski, M.A., 2009. Empirical models of toxigenic *Pseudo-nitzschia* blooms: potential use as a remote detection tool in the Santa Barbara Channel. Harmful Algae 8 (3), 478–492.
Anderson, C.R., Kudela, R.M., Benitez-Nelson, C., Sekula-Wood, E., Burrell, C.T., Chao, Y., Langlois, G., Goodman, J., Siegel, D.A., 2011. Detecting toxic diatom blooms from ocean color and a regional ocean model. Geophys. Res. Lett. 38 (4).
Anderson, C.R., Kudela, R.M., Kahru, M., Chao, Y., Rosenfeld, L.K., Bahr, F.L., Anderson, D.M., Norris, T.A., 2016. Initial skill assessment of the California Harmful Algae Risk Mapping (C-HARM) system. Harmful Algae, 59, 1–18.
Anderson, D.M., Fensin, E., Gobler, C.J., Hoeglund, A.E., Hubbard, K.A., Kulis, D.M., Landsberg, J.H., Lefebvre, K.A., Provoost, P., Richlen, M.L., Smith, J.L., Solow, A.R., Trainer, V.L., 2021. Marine harmful algal blooms (HABs) in the United States: history, current status and future trends. Harmful Algae 102.
Arapov, J., Bužančič, M., Skejič, S., Mandič, J., Bakrač, A., Straka, M., Gladan, Ž.N., 2020. Phytoplankton dynamics in the middle adriatic estuary, with a focus on the potentially toxic genus *Pseudo-nitzschia*. J. Mar. Sci. Eng. 8 (8).
Bargu, S., Baustian, M.M., Rabalais, N.N., Del Rio, R., Von Korff, B., Turner, R.E., 2016. Influence of the Mississippi River on *Pseudo-nitzschia* spp. Abundance and toxicity in Louisiana coastal waters. Estuaries Coasts 39 (5), 1345–1356.
Barron, J.A., Bukry, D., Field, D., 2010. Santa Barbara Basin diatom and silicoflagellate response to global climate anomalies during the past 2200 years. Quat. Int. 215 (1–2), 34–44.
Barron, J.A., Bukry, D., Field, D.B., Finney, B., 2013. Response of diatoms and silicoflagellates to climate change and warming in the California Current during the past 250 years and the recent rise of the toxic diatom *Pseudo-nitzschia australis*. Quat. Int. 310, 140–154.
Bates, S.S., Bird, C.J., Freitas, A.D., Foxall, R., Gilgan, M., Hanic, L.A., Johnson, G.R., McCulloch, A.W., Odense, P., Pocklington, R., Quilliam, M.A., Sim, P.G., Smith, J.C., Subba Rao, D.V., Todd, E.C.D., Walter, J.A., Wright, J.L.C., 1989. Pennate diatom *Nitzschia pungens* as the primary source of domoic acid, a toxin in shellfish from eastern Prince Edward Island, Canada. Can. J. Fish. Aquat. Sci. 46 (7), 1203–1215.
Bates, S.S., Hubbard, K.A., Lundholm, N., Montresor, M., Leaw, C.P., 2018. *Pseudo-nitzschia, Nitzschia*, and domoic acid: new research since 2011. Harmful Algae 79 (October), 3–43.
Bejarano, A.C., VanDola, F.M., Gulland, F.M., Rowles, T.K., Schwacke, L.H., 2008. Production and toxicity of the marine biotoxin domoic acid and its effects on wildlife: a review. HERA 14 (3), 544–567.
Bernstein, S., Ruiz-Cooley, R.I., Kudela, R., Anderson, C.R., Dunkin, R., Field, J.C., 2021. Stable isotope analysis reveals differences in domoic acid accumulation and feeding strategies of key vectors in a California hotspot for outbreaks. Harmful Algae 110 (April), 102117.
Bowers, H.A., Ryan, J.P., Hayashi, K., Woods, A.L., Marin, R., Smith, G.J., Hubbard, K.A., Doucette, G.J., Mikulski, C.M., Gellene, A.G., Zhang, Y., Kudela, R.M., Caron, D.A., Birch, J.M., Scholin, C.A., 2018. Diversity and toxicity of *Pseudo-nitzschia* species in Monterey Bay: perspectives from targeted and adaptive sampling. Harmful Algae 78, 129–141.
Bricker, S.B., Ferreira, J.G., Simas, T., 2003. An integrated methodology for assessment of estuarine trophic status. Ecol. Modell. 169 (1), 39–60.
Bricker, S.B., Longstaff, B., Dennison, W., Jones, A., Boicourt, K., Wicks, C., Woerner, J., 2008. Effects of nutrient enrichment in the nation's estuaries: a decade of change. Harmful Algae 8 (1), 21–32.
Brzezinski, M.A., Washburn, L., 2011. Phytoplankton primary productivity in the Santa Barbara Channel: effects of wind-driven upwelling and mesoscale eddies. J. Geophys. Res. Oceans 116 (12).
Catlett, D., Siegel, D.A., Simons, R.D., Guillocheau, N., Henderikx-Freitas, F., Thomas, C. S., 2021. Diagnosing seasonal to multi-decadal phytoplankton group dynamics in a highly productive coastal ecosystem. Prog. Oceanogr. 197.
Chai, Z.Y., Wang, H., Deng, Y., Hu, Z., Zhong Tang, Y., 2020. Harmful algal blooms significantly reduce the resource use efficiency in a coastal plankton community. Sci. Total. Environ. 704, 135381.
Chavez, F.P., Pennington, J.T., Castro, C.G., Ryan, J.P., Michisaki, R.P., Schlining, B., Walz, P., Buck, K.R., McFadyen, A., Collins, C.A., 2002. Biological and chemical consequences of the 1997-1998 El Niño in central California waters. Prog. Oceanogr. 54 (1–4), 205–232.
Chavez, F.P., Pennington, J.T., Michisaki, R.P., Blum, M., Chavez, G.M., Friederich, J., Jones, B., Herlien, R., Kieft, B., Hobson, B., Ren, A.S., Ryan, J., Sevadjian, J.C., Wahl, C., Walz, K.R., Yamahara, K., Friederich, G.E., Messié, M., 2017. Climate variability and change: response of a coastal ocean ecosystem. Oceanogr. 30 (4), 128–145.
Chavez, F.P., Min, M., Pitz, K., Truelove, N., Baker, J., LaScala-Grunewald, D., Blum, M., Walz, K., Nye, C., Djurhuus, A., Miller, R.J., Goodwin, K.D., Muller-Karger, F.E., Ruhl, H.A., Scholin, C.A., 2021. Observing life in the sea using environmental DNA. Oceanogr. 34 (2), 102–119.
Clark, S., Hubbard, K.A., Anderson, D.M., McGillicuddy, D.J., Ralston, D.K., Townsend, D.W., 2019. *Pseudo-nitzschia* bloom dynamics in the Gulf of Maine: 2012–2016. Harmful Algae 88 (May), 101656.
Cochlan, W.P., Herndon, J., Kudela, R.M., 2008. Inorganic and organic nitrogen uptake by the toxigenic diatom *Pseudo-nitzschia australis* (Bacillariophyceae). Harmful Algae 8 (1), 111–118.
Córdoba-Mena, N., Florez-Leiva, L., Atehortúa, L., Obando, E., 2020. Changes in phytoplankton communities in a tropical estuary in the Colombian Caribbean sea. Estuaries Coasts 43 (8), 2106–2127.
Dale, B., Edwards, M., Reid, P.C., 2006. Climate change and harmful algal blooms. Ecol. Harmful Algae 189, 367–378.
Delegrange, A., Lefebvre, A., Gohin, F., Courcot, L., Vincent, D., 2018. *Pseudo-nitzschia* sp. diversity and seasonality in the southern North Sea, domoic acid levels and associated phytoplankton communities. Estuar. Coast. Shelf Sci. 214 (April), 194–206.
Devlin, M., Bricker, S., Painting, S., 2011. Comparison of five methods for assessing impacts of nutrient enrichment using estuarine case studies. Biogeochemistry 106 (2), 177–205.
DiGiacomo, P.M., Holt, B., 2001. Satellite observations of small coastal ocean eddies in the Southern California Bight. J. Geophys. Res. Oceans 106 (C10), 22521–22543.
Di Lorenzo, E., Schneider, N., Cobb, K.M., Franks, P.J.S., Chhak, K., Miller, A.J., McWilliams, J.C., Bograd, S.J., Arango, H., Curchitser, E., Powell, T.M., Rivière, P., 2008. North Pacific Gyre Oscillation links ocean climate and ecosystem change. Geophys. Res. Lett. 35 (8), 2–7.
Dortch, Q., Robichaux, R., Pool, S., Milsted, D., Mire, G., Rabalais, N.N., Soniat, T.M., Fryxell, G.A., Turner, R.E., Parsons, M.L., 1997. Abundance and vertical flux of *Pseudo-nitzschia* in the northern Gulf of Mexico. Mar Ecol Prog Ser 146 (1–3), 249–264.
Doucette, G.J., King, K.L., Thessen, A.E., Dortch, Q., 2008. The effect of salinity on domoic acid production by the diatom *Pseudo-nitzschia multiseries*. Nova Hedwigia 133 (31), 1439-0485.
Du, X., Peterson, W., Fisher, J., Hunter, M., Peterson, J., 2016. Initiation and development of a toxic and persistent *Pseudo-nitzschia* bloom off the Oregon coast in spring/summer2015. PLoS ONE 11 (10).
Gai, F.F., Hedemand, C.K., Louw, D.C., Grobler, K., Krock, B., Moestrup, Ø., Lundholm, N., 2018. Morphological, molecular, and toxigenic characteristics of Namibian *Pseudo-nitzschia* species – including *Pseudo-nitzschia bucculenta* sp. nov. Harmful Algae 76 (May), 80–95.
Garali, S.M.B., Sahraoui, I., de la Iglesia, P., Chalghaf, M., Diogène, J., Ksouri, J., Sakka Hlaili, A., 2020. Factors driving the seasonal dynamics of *Pseudo-nitzschia* species and domoic acid at mussel farming in the SW Mediterranean Sea. Chem. Ecol. 36 (1), 66–82.
Gárate-Lizárraga, I., Band-Schmidt, C.J., López-Cortés, D.J., Bustillos-Guzmán, J.J., Erler, K., 2007. Bloom of *Pseudo-nitzschia fraudulenta* in Bahía de La Paz, Gulf of California (june-july 2006). Harmful Algae News 33, 6–7.
García-Mendoza, E., Rivas, D., Olivos-Ortiz, A., Almazán-Becerril, A., Castañeda-Vega, C., Peña-Manjarrez, J.L., 2009. A toxic *Pseudo-nitzschia* bloom in Todos Santos Bay, northwestern Baja California, Mexico. Harmful Algae 8 (3), 493–503.
Gibble, C.M., Kudela, R.M., Knowles, S., Bodenstein, B., Lefebvre, K.A., 2021. Domoic acid and saxitoxin in seabirds in the United States between 2007 and 2018. Harmful Algae 103.
Graham, W.M., 1993. Spatio-temporal scale assessment of an "upwelling shadow" in northern Monterey Bay, California. Estuaries. 16 (1), 83–91.
Harding, L.W., Batiuk, R.A., Fisher, T.R., Gallegos, C.L., Malone, T.C., Miller, W.D., Mulholland, M.R., Paerl, H.W., Perry, E.S., Tango, P., 2014. Scientific bases for numerical chlorophyll criteria in Chesapeake Bay. Estuaries Coasts 37 (1), 134–148.
Harms, S., Winant, C.D., 1998. Characteristic patterns of the circulation in the Santa Barbara Channel. J. Geophys. Res. Oceans 103 (C2), 3041–3065.
Henson, S.A., Thomas, A.C., 2007. Phytoplankton scales of variability in the California Current System: 1. Interannual and cross-shelf variability. J. Geophys. Res. Oceans 112 (7).
Hickey, B.M., 1992. Circulation over the Santa Monica-San Pedro Basin and Shelf. Prog. Oceanogr. 30 (1–4), 37–115.
Hoffmeyer, M.S., Dutto, M.S., Berasategui, A.A., Garcia, M.D., Pettigrosso, R.E., Almandoz, G.O., D'Agostino, V., García, T.M., Fabro, E., Paparazzo, F.E., Solís, M., Williams, G., Esteves, J.L., Krock, B, 2020. Domoic acid, *Pseudo-nitzschia* spp and potential vectors at the base of the pelagic food web over the northern Patagonian coast, Southwestern Atlantic. J. Mar. Syst. 212 (August), 103448.
Horner, R.A., Postel, J.R., 1993. Toxic diatoms in western Washington waters (US west coast). In: Twelfth International Diatom Symposium. Dordrecht. Springer, pp. 197–205.
Howard, M.D.A., Cochlan, W.P., Ladizinsky, N., Kudela, R.M., 2007. Nitrogenous preference of toxigenic *Pseudo-nitzschia australis* (Bacillariophyceae) from field and laboratory experiments. Harmful Algae 6 (2), 206–217.
Howard, M.D.A., Sutula, M., Caron, D.A., Chao, Y., Farrara, J.D., Frenzel, H., Jones, B., Robertson, G., McLaughlin, K., Sengupta, A., 2014. Anthropogenic nutrient sources rival natural sources on small scales in the coastal waters of the Southern California Bight. Limnol. Oceanogr. 59 (1), 285–297.
Howes, E.L., Joos, F., Eakin, C.M., Gattuso, J.P., 2015. An updated synthesis of the observed and projected impacts of climate change on the chemical, physical and biological processes in the oceans. In: Front in Marine Science, 2. Front Media S. A (Jun).
Husson, B., Hernández-Fariñas, T., Le Gendre, R., Schapira, M., Chapelle, A., 2016. Two decades of *Pseudo-nitzschia* spp. blooms and king scallop (*Pecten maximus*) contamination by domoic acid along the French Atlantic and English Channel coasts: seasonal dynamics, spatial heterogeneity and interannual variability. Harmful Algae 51, 26–39.
Jacox, M.G., Fiechter, J., Moore, A.M., Edwards, C.A., 2015. ENSO and the California Current coastal upwelling response. J. Geophys. Res. Oceans 120 (3), 1691–1702.
Jester, R., Lefebvre, K., Langlois, G., Vigilant, V., Baugh, K., Silver, M.W., 2009. A shift in the dominant toxin-producing algal species in central California alters phycotoxins in food webs. Harmful Algae 8 (2), 291–298.

Kessouri, F., McWilliams, J.C., Bianchi, D., Sutula, M., Renault, L., Deutsch, C., Feely, R. A., McLaughlin, K., Ho, M., Howard, E.M., Bednarsek, N., Damien, P., Molemaker, J, Weisberg, S.B., 2021a. Coastal eutrophication drives acidification, oxygen loss, and ecosystem change in a major oceanic upwelling system. PNAS 118 (21), e2018856118.

Kessouri, F., McLaughlin, K., Sutula, M.A., Bianchi, D., Ho, M., McWilliams, J.C., Renault, L., Molemaker, J., Deutsch, C.A., Leinweber, A., 2021b. Configuration and validation of an oceanic physical and biogeochemical model to investigate coastal eutrophication: case study in the Southern California Bight. J. Adv. Model Earth Syst. 13 (12), e2020MS002296.

Kessouri, F., Renault, L., McWilliams, J.C., Damien, P., Bianchi, D., 2022. Enhancement of oceanic eddy activity by fine-scale orographic winds drives high productivity, low oxygen, and low pH conditions in the Santa Barbara Channel. J. Geophys. Res. Oceans. 127 (12).

Kelchner, H., Reeve-Arnold, K.E., Schreiner, K.M., Bargu, S., Roques, K.G., Errera, R.M., 2021. Domoic Acid and *Pseudo-nitzschia* spp. Connected to Coastal Upwelling along Coastal Inhambane Province, Mozambique: a New Area of Concern. Toxins (Basel) 13 (12), 903.

Kotaki, Y., Koike, K., Sato, S., Ogata, T., Fukuyo, Y., Kodama, M., 1999. Confirmation of domoic acid production of *Pseudo-nitzschia multiseries* isolated from Ofunato Bay. Japan. Toxicon 37 (4), 677–682.

Kudela, R.M., Dugdale, R.C., 2000. Nutrient regulation of phytoplankton productivity in Monterey Bay, California. Deep Sea Res. 2 Top. Stud. Oceanogr. 47 (5–6), 1023–1053.

Kudela, R., Roberts, A., Armstrong, M., 2002. Laboratory analyses of nutrient stress and toxin production in *Pseudo-nitzschia* spp. from Monterey Bay, California. Harmful Algae 136–138.

Kudela, R.M., Cochlan, W.P., 2003. Spatial and temporal patterns of *Pseudo-nitzschia* spp. in central California related regional oceanography. Harmful Algae 347–349.

Kudela, R.M., Lane, J.Q., Cochlan, W.P., 2008. The potential role of anthropogenically derived nitrogen in the growth of harmful algae in California, USA. Harmful Algae 8 (1), 103–110.

Kvrgić, K., Lešić, T., Džafić, N., Pleadin, J., 2022. Occurrence and seasonal monitoring of domoic acid in three shellfish species from the northern Adriatic Sea. Toxins (Basel) 14 (1).

Lane, J.Q., Raimondi, P.T., Kudela, R.M., 2009. Development of a logistic regression model for the prediction of toxigenic *Pseudo-nitzschia* blooms in Monterey Bay, California. Mar Ecol Prog Ser 383, 37–51.

Lefebvre, K.A., Robertson, A., 2010. Domoic acid and human exposure risks: a review. Toxicon 56 (2), 218–230.

Lelong, A., Hégaret, H., Soudant, P., Bates, S.S., 2012. *Pseudo-nitzschia* (Bacillariophyceae) species, domoic acid and amnesic shellfish poisoning: revisiting previous paradigms. Phycologia 51 (2), 168–216.

Lewitus, A.J., Horner, R.A., Caron, D.A., Garcia-Mendoza, E., Hickey, B.M., Hunter, M., Huppert, D.D., Kudela, R.M., Langlois, G.W., Largier, J.L., Lessard, E.J., RaLonde, R., Jack Rensel, J.E., Strutton, P.G., Trainer, V.L., Tweddle, J.F., 2012. Harmful algal blooms along the North American west coast region: history, trends, causes, and impacts. Harmful Algae 19, 133–159.

Liefer, J.D., Robertson, A., MacIntyre, H.L., Smith, W.L., Dorsey, C.P., 2013. Characterization of a toxic *Pseudo-nitzschia* spp. bloom in the Northern Gulf of Mexico associated with domoic acid accumulation in fish. Harmful Algae 26, 20–32.

Likumahua, S., de Boer, M.K., Krock, B., Nieuwenhuizen, T., Tatipatta, W.M., Hehakaya, S., Imu, L., Abdul, M.S., Moniharapon, E., Buma, A.G.J., 2019. First record of the dynamics of domoic acid producing *Pseudo-nitzschia* spp. in Indonesian waters as a function of environmental variability. Harmful Algae 90 (November), 101708.

Lundholm, N., Krock, B., John, U., Skov, J., Cheng, J., Pančić, M., Wohlrab, S., Rigby, K., Nielsen, T.G., Selander, E., Harðardóttir, S., 2018. Induction of domoic acid production in diatoms—Types of grazers and diatoms are important. Harmful Algae 79 (August), 64–73.

Macintyre, H.L., Stutes, A.L., Smith, W.L., Dorsey, C.P., Annabraham, Dickey, R.W., 2011. Environmental correlates of community composition and toxicity during a bloom of *Pseudo-nitzschia* spp. in the northern Gulf of Mexico. J. Plankton Res. 33 (2), 273–295.

Maldonado, M.T., Hughes, M.P., Rue, E.L., Wells, M.L., 2002. The effect of Fe and Cu on growth and domoic acid production by *Pseudo-nitzschia multiseries* and *Pseudo-nitzschia australis*. Limnol. Oceanogr. 47 (2).

Mantua, N.J., Hare, S.R., Zhang, Y., Wallace, J.M., Francis, R.C., 1997. A pacific interdecadal climate oscillation with impacts on salmon production. Bull. Am. Meteorol. Soc. 78 (6), 1069–1079.

Mantua, N.J., H, 2002. The pacific decadal oscillation. J. Oceanogr. 58, 35–44.

McCabe, R.M., Hickey, B.M., Kudela, R.M., Lefebvre, K.A., Adams, N.G., Bill, B.D., Gulland, F.M.D., Thomson, R.E., Cochlan, W.P., Trainer, V.L., 2016. An unprecedented coastwide toxic algal bloom linked to anomalous ocean conditions. Geophys. Res. Lett. 43 (19), 10,366-10,376.

McManus, M.A., Kudela, R.M., Silver, M.W., Steward, G.F., Donaghay, P.L., Sullivan, J. M., 2008. Cryptic blooms: are thin layers the missing connection? Estuaries Coasts 31 (2), 396–401.

McManus, M.A., Greer, A.T., Timmerman, A.H.V., Sevadjian, J.C., Woodson, C.B., Cowen, R., Fong, D.A., Monismith, S., Cheriton, O.M., 2021. Characterization of the biological, physical, and chemical properties of a toxic thin layer in a temperate marine system. Mar. Ecol. Prog. Ser. 678, 17–35.

McKibben, S.M., Peterson, W., Wood, A.M., Trainer, V.L., Hunter, M., White, A.E., 2017. Climatic regulation of the neurotoxin domoic acid. PNAS 114 (2), 239–244.

Moore, S.K., Dreyer, S.J., Ekstrom, J.A., Moore, K., Norman, K., Klinger, T., Allison, E.H., Jardine, S.L., 2020. Harmful algal blooms and coastal communities: socioeconomic impacts and actions taken to cope with the 2015 U.S. West Coast domoic acid event. Harmful Algae 96.

Moreno, A.R., Anderson, C., Kudela, R.M., Sutula, M., Edwards, C., Bianchi, D., 2022. Development, calibration, and evaluation of a model of *Pseudo-nitzschia* and domoic acid production for regional ocean modeling studies. Harmful Algae 118 (July), 102296.

Moriarty, M.E., Tinker, M.T., Miller, M.A., Tomoleoni, J.A., Staedler, M.M., Fujii, J.A., Batac, F.I., Dodd, E.M., Kudela, R.M., Zubkousky-White, V., Johnson, C.K., 2021. Exposure to domoic acid is an ecological driver of cardiac disease in southern sea otters. Harmful Algae 101.

Palma, S., Mouriño, H., Silva, A., Barão, M.I., Moita, M.T., 2010. Can *Pseudo-nitzschia* blooms be modeled by coastal upwelling in Lisbon Bay? Harmful Algae 9 (3), 294–303.

Pan, Y., Bates, S.S., Cembella, A.D., 1998. Environmental stress and domoic acid production by *Pseudo-nitzschia*: a physiological perspective. Nat. Toxins. 6 (3–4), 127–135.

Perl, T.M., Bedard, L., Kosatsky, T., Hockin, J.C., Todd, E.C., Remis, R.S., 1990. An outbreak of toxic encephalopathy caused by eating mussels contaminated with domoic acid. New Engl. J. Medic. 322 (25), 1775–1780.

Pitcher, G.C., Cembella, A.D., Krock, B., Macey, B.M., Mansfield, L., 2020. Do toxic *Pseudo-nitzschia* species pose a threat to aquaculture in the southern Benguela eastern boundary upwelling system? Harmful Algae 99 (June), 101919.

Qi, Y., 1994. The taxonomy and bloom ecology of *Pseudo-nitzschia* on the coasts of China. In: Proceedings IOC-WESTPAC Third International Scientific Symposium. Bali, Indonesia, pp. 88–95, 22-26 Nov.

Radan, R.L., Cochlan, W.P., 2018. Differential toxin response of *Pseudo-nitzschia multiseries* as a function of nitrogen speciation in batch and continuous cultures, and during a natural assemblage experiment. Harmful Algae 73, 12–29.

Renault, L., McWilliams, J.C., Kessouri, F., Jousse, A., Frenzel, H., Chen, R., Deutsch, C., 2021. Evaluation of high-resolution atmospheric and oceanic simulations of the California Current System. Prog. Oceanogr. 195, 102564.

Rines, J.E.B., McFarland, M.N., Donaghay, P.L., Sullivan, J.M., 2010. Thin layers and species-specific characterization of the phytoplankton community in Monterey Bay, California, USA. Cont. Shelf. Res. 30 (1), 66–80.

Ryan, J.P., McManus, M.A., Kudela, R.M., Lara Artigas, M., Bellingham, J.G., Chavez, F. P., Doucette, G., Foley, D., Godin, M., Harvey, J.B.J., Marin, R., Messié, M., Mikulski, C., Pennington, T., Py, F., Rajan, K., Shulman, I., Wang, Z., Zhang, Y., 2014. Boundary influences on HAB phytoplankton ecology in a stratification-enhanced upwelling shadow. Deep Sea Res. 2 Top. Stud. Oceanogr. 101, 63–79.

Ryan, J.P., Kudela, R.M., Birch, J.M., Blum, M., Bowers, H.A., Chavez, F.P., Doucette, G. J., Hayashi, K., Marin, R., Mikulski, C.M., Pennington, J.T., Scholin, C.A., Smith, G. J., Woods, A., Zhang, Y., 2017. Causality of an extreme harmful algal bloom in Monterey Bay, California, during the 2014–2016 northeast Pacific warm anomaly. Geophys. Res. Lett. 44 (11), 5571–5579.

Schnetzer, A., Miller, P.E., Schaffner, R.A., Stauffer, B.A., Jones, B.H., Weisberg, S.B., DiGiacomo, P.M., Berelson, W.M., Caron, D.A., 2007. Blooms of *Pseudo-nitzschia* and domoic acid in the San Pedro Channel and Los Angeles harbor areas of the Southern California Bight, 2003-2004. Harmful Algae 6 (3), 372–387.

Schnetzer, A., Jones, B.H., Schaffner, R.A., Cetinic, I., Fitzpatrick, E., Miller, P.E., Seubert, E.L., Caron, D.A., 2013. Coastal upwelling linked to toxic *Pseudo-nitzschia australis* blooms in Los Angeles coastal waters, 2005-2007. J. Plankton Res. 35 (5), 1080–1092.

Scholin, C.A., Gulland, F., Doucette, G.J., Benson, S., Busman, M., Chavez, F.P., Cordaro, J., DeLong, R., De Vogelaere, A., Harvey, J., Haulena, M., Lefebvre, K., Lipscomb, T., Loscutoff, S., Lowenstine, L.J., Marin, R., Miller, P.E., McLellan, W.A., Moeller, P.D.R., Van Dolah, F.M., 2000. Mortality of sea lions along the central California coast linked to a toxic diatom bloom. Nature 403 (6765), 80–84.

Seegers, B.N., Birch, J.M., Marin, R., Scholin, C.A., Caron, D.A., Seubert, E.L., Howard, M.D.A., Robertson, G.L., Jones, B.H., 2015. Subsurface seeding of surface harmful algal blooms observed through the integration of autonomous gliders, moored environmental sample processors, and satellite remote sensing in southern California. Limnol. Oceanogr. 60 (3), 754–764.

Sekula-Wood, E., Benitez-Nelson, C., Morton, S., Anderson, C., Burrell, C., Thunell, R., 2011. *Pseudo-nitzschia* and domoic acid fluxes in Santa Barbara Basin (CA) from 1993 to 2008. Harmful Algae 10 (6), 567–575.

Seubert, E.L., Gellene, A.G., Howard, M.D.A., Connell, P., Ragan, M., Jones, B.H., Runyan, J., Caron, D.A., 2013. Seasonal and annual dynamics of harmful algae and algal toxins revealed through weekly monitoring at two coastal ocean sites off southern California, USA. Environ. Sci. Pollut. Res. 20 (10), 6878–6895.

Shipe, R.F., Leinweber, A., Gruber, N., 2008. Abiotic controls of potentially harmful algal blooms in Santa Monica Bay, California. Cont. Shelf. Res. 28 (18), 2584–2593.

Sison-Mangus, M.P., Jiang, S., Tran, K.N., Kudela, R.M., 2014. Host-specific adaptation governs the interaction of the marine diatom, *Pseudo-nitzschia* and their microbiota. ISME 8 (1), 63–76.

Smith, J.C., Cormier, R., Worms, J., Bird, C.J., Quilliam, M.A., Pocklington, R., Angus, R., Hanic, L.A., 1990. Toxic blooms of the domoic acid containing diatom *Nitzschia pungens* in the Cardigan River Prince Edward Island Canada in 1988. In: Toxic Marine Phytoplankton; proceedings of the Fourth International Conference on Marine Phytoplankton, held June 26-30 in Lund. Sweden, pp. 227–232.

Smith, J., Connell, P., Evans, R.H., Gellene, A.G., Howard, M.D.A., Jones, B.H., Kaveggia, S., Palmer, L., Schnetzer, A., Seegers, B.N., Seubert, E.L., Tatters, A.O., Caron, D.A., 2018a. A decade and a half of *Pseudo-nitzschia* spp. and domoic acid along the coast of southern California. Harmful Algae 79, 87–104.

Smith, J., Gellene, A.G., Hubbard, K.A., Bowers, H.A., Kudela, R.M., Hayashi, K., Caron, D.A., 2018b. *Pseudo-nitzschia* species composition varies concurrently with

domoic acid concentrations during two different bloom events in the Southern California Bight. J. Plankton Res. 40 (1), 1–17.
Spatharis, S., Danielidis, D.B., Tsirtsis, G., 2007. Recurrent *Pseudo-nitzschia calliantha* (Bacillariophyceae) and *Alexandrium insuetum* (Dinophyceae) winter blooms induced by agricultural runoff. Harmful Algae 6 (6), 811–822.
Subba Rao, D.V., Quilliam, M.A., Pocklington, R., 1988. Domoic acid - A neurotoxic amino acid produced by the marine diatom *Nitzschia pungens* in culture. Can. J. Fish. Aquat. Sci. 45 (12), 2076–2079.
Sutula, M., Senn, D. 2017. Scientific bases for assessment of nutrient impacts on San Francisco Bay. Southern California coastal water research project authority technical report 864. www.sccwrp.org, 56 pp.
Sutula, M., Kudela, R., Hagy, J.D., Harding, L.W., Senn, D., Cloern, J.E., Bricker, S., Berg, G.M., Beck, M., 2017. Novel analyses of long-term data provide a scientific basis for chlorophyll-a thresholds in San Francisco Bay. Estuar. Coast. Shelf Sci. 197, 107–118.
Sutula, M., Ho, M., Sengupta, A., Kessouri, F., McLaughlin, K., McCune, K., Bianchi, D., 2021. A baseline of terrestrial freshwater and nitrogen fluxes to the Southern California Bight, USA. Mar. Pollut. Bull. 170, 112669.
Tatters, A.O., Fu, F.X., Hutchins, D.A., 2012. High CO 2 and silicate limitation synergistically increase the toxicity of *Pseudo-nitzschia fraudulenta*. PLoS ONE 7 (2).
Taylor, F.J.R., Horner, R.A., 1994. Red tides and other problems with harmful algal blooms in Pacific Northwest coastal waters. In: Review of the Marine Environment and Biota of Strait of Georgia, Puget Sound and Juan de Fuca Strait: Proceedings of the BC/Washington Symposium on the Marine Environment. Can. Tech. Rep. Fish. Aquat. Sci, pp. 175–186, 1948.
Thorel, M., Fauchot, J., Morelle, J., Raimbault, V., Le Roy, B., Miossec, C., Kientz-Bouchart, V., Claquin, P., 2014. Interactive effects of irradiance and temperature on growth and domoic acid production of the toxic diatom *Pseudo-nitzschia australis* (Bacillariophyceae). Harmful Algae 39, 232–241.
Thorel, M., Claquin, P., Schapira, M., Le Gendre, R., Riou, P., Goux, D., Le Roy, B., Raimbault, V., Deton-Cabanillas, A.F., Bazin, P., Kientz-Bouchart, V., Fauchot, J., 2017. Nutrient ratios influence variability in *Pseudo-nitzschia* species diversity and particulate domoic acid production in the Bay of Seine (France). Harmful Algae 68, 192–205.
Timmerman, A.H.V., McManus, M.A., Cheriton, O.M., Cowen, R.K., Greer, A.T., Kudela, R.M., Ruttenberg, K., Sevadjian, J., 2014. Hidden thin layers of toxic diatoms in a coastal bay. Deep Sea Res. 2 Top. Stud. Oceanogr. 101, 129–140.
Trainer, V.L., Adams, N.G., Bill, B.D., Anulacion, B.F., Wekell, J.C., 1998. Concentration and dispersal of a *Pseudo-nitzschia* bloom in Penn Cove, Washington, USA. Nat. Toxins. 6 (3–4), 113–125.
Trainer, V.L., Adams, N.G., Bill, B.D., Stehr, C.M., Wekell, J.C., Moeller, P., Busman, M., Woodruff, D., 2000. Domoic acid production near California coastal upwelling zones, June 1998. Limnol. Ocean. 45 (8), 1818–1833.
Trainer, V.L., Hickey, B.M., Bates, S.S. 2008. Toxic diatoms. Oceans and human health: risks and remedies from the sea. In P.J. Walsh, S.L. Smith, L.E. Fleming, H. Solo-Gabriele, W.H. Gerwick (eds). New york. 14, 219–237.
Trainer, V.L., Hickey, B.M., Lessard, E.J., Cochlan, W.P., Trick, C.G., Wells, M.L., MacFadyen, A., Moore, S.K., 2009. Variability of *Pseudo-nitzschia* and domoic acid in the Juan de Fuca eddy region and its adjacent shelves. Limnol. Oceanogr. 54 (1), 289–308.
Trainer, V.L., Pitcher, G.C., Reguera, B., Smayda, T.J., 2010. The distribution and impacts of harmful algal bloom species in eastern boundary upwelling systems. Prog. Oceanogr. 85 (1–2), 33–52.
Trainer, V.L., Bates, S.S., Lundholm, N., Thessen, A.E., Cochlan, W.P., Adams, N.G., Trick, C.G., 2012. *Pseudo-nitzschia* physiological ecology, phylogeny, toxicity, monitoring and impacts on ecosystem health. Harmful Algae 14, 271–300.
Trainer, V.L., Moore, S.K., Hallegraeff, G., Kudela, R.M., Clement, A., Mardones, J.I., Cochlan, W.P., 2020a. Pelagic harmful algal blooms and climate change: lessons from nature's experiments with extremes. Harmful Algae 91.
Trainer, V.L., Kudela, R.M., Hunter, M.V., Adams, N.G., McCabe, R.M., 2020b. Climate extreme seeds a new domoic acid hotspot on the US West Coast. Front. Clim. 2, 571836.
Ujevic, I., Nincevic-Gladan, Ž., Roje, R., Skejic, S., Arapov, J., Marasovic, I., 2010. Domoic acid-A new toxin in the croatian adriatic shellfish toxin profile. Molecules 15 (10), 6835–6849.
Umhau, B.P., Benitez-Nelson, C.R., Anderson, C.R., McCabe, K., Burrell, C., 2018. A time series of water column distributions and sinking particle flux of *Pseudo-nitzschia* and domoic acid in the Santa Barbara Basin, California. Toxins (Basel) 10 (11).
Van Meerssche, E., Pinckney, J.L., 2017. The influence of salinity in the domoic acid effect on estuarine phytoplankton communities. Harmful Algae 69, 65–74.
Velo-Suárez, L., González-Gil, S., Gentien, P., Lunven, M., Bechemin, C., Fernand, L., Raine, R., Reguera, B., 2008. Thin layers of *Pseudo-nitzschia* spp. and the fate of *Dinophysis acuminata* during an upwelling-downwelling cycle in a Galician Ría. Limnol. Oceanogr. 53 (5), 1816–1834.
Wang, Y., Wang, T., Zhuang, J., 2018. Modeling continuous time series with many zeros and an application to earthquakes. Environmetrics 29 (4), 1–21.
Wells, M.L., Trick, C.G., Cochlan, W.P., Hughes, M.P., Trainer, V.L., 2005. Domoic acid: the synergy of iron, copper, and the toxicity of diatoms. Limnol. Oceanogr. 50 (6), 1908–1917.
Wells, M.L., Karlson, B., Wulff, A., Kudela, R., Trick, C., Asnaghi, V., Berdalet, E., Cochlan, W., Davidson, K., De Rijcke, M., Dutkiewicz, S., Hallegraeff, G., Flynn, K.J., Legrand, C., Paerl, H., Silke, J., Suikkanen, S., Thompson, P., Trainer, V.L., 2020. Future HAB science: directions and challenges in a changing climate. Harmful Algae 91.
Wingert, C.J., Cochlan, W.P., 2021. Effects of ocean acidification on the growth, photosynthetic performance, and domoic acid production of the diatom *Pseudo-nitzschia australis* from the California Current System. Harmful Algae 107.
Wood, S., Bill, B.D., Trainer, V.L., 2017. Variability of *Pseudo-nitzschia* and Domoic Acid Along the US West Coast. In: AGU Fall Meeting Abstracts, 2017, pp. OS23A–O1370.
Zaldívar, J., Cardoso, A.C., Viaroli, P., Wit, R.De, Ibañez, C., Reizopoulou, S., Razinkovas, A., Basset, A., Holmer, M., Murray, N., 2008. Eutrophication in transitional waters : an overview. TWM, Transit. Waters Monogr. 1, 1–78.
Zou, J.Z., Zhou, M.J., Zhang, C., 1993. Ecological Features of Toxic *Nitzschia pungens* Grunow in Chinese coastal waters. Toxic phytoplankton Blooms in the Sea. Elsevier Sci. Publ. BV, Amsterdam, pp. 651–657.
Zuur, A.F., Leno, E.N., Walker, N.J., Saveliev, A.A., Smith, G.M., 2009. Mixed Effects Models and Extensions in Ecology With R (574). Springer, New York.